Journal of Anatomy

J. Anat. (2019) **235**, pp45–66 doi: 10.1111/joa.12966

Metacarpal trabecular bone varies with distinct hand-positions used in hominid locomotion

Christopher J. Dunmore,[1] Tracy L. Kivell,[1,2] Ameline Bardo[1] and Matthew M. Skinner[1,2]

[1]*Skeletal Biology Research Centre, School of Anthropology and Conservation, University of Kent, Canterbury, UK*
[2]*Department of Human Evolution, Max Planck Institute for Evolutionary Anthropology, Leipzig, Germany*

Abstract

Trabecular bone remodels during life in response to loading and thus should, at least in part, reflect potential variation in the magnitude, frequency and direction of joint loading across different hominid species. Here we analyse the trabecular structure across all non-pollical metacarpal distal heads (Mc2-5) in extant great apes, expanding on previous volume of interest and whole-epiphysis analyses that have largely focused on only the first or third metacarpal. Specifically, we employ both a univariate statistical mapping and a multivariate approach to test for both inter-ray and interspecific differences in relative trabecular bone volume fraction (RBV/TV) and degree of anisotropy (DA) in Mc2-5 subchondral trabecular bone. Results demonstrate that whereas DA values only separate *Pongo* from African apes (*Pan troglodytes, Pan paniscus, Gorilla gorilla*), RBV/TV distribution varies with the predicted loading of the metacarpophalangeal (McP) joints during locomotor behaviours in each species. *Gorilla* exhibits a relatively dorsal distribution of RBV/TV consistent with habitual hyper-extension of the McP joints during knuckle-walking, whereas *Pongo* has a palmar distribution consistent with flexed McP joints used to grasp arboreal substrates. Both *Pan* species possess a disto-dorsal distribution of RBV/TV, compatible with multiple hand postures associated with a more varied locomotor regime. Further inter-ray comparisons reveal RBV/TV patterns consistent with varied knuckle-walking postures in *Pan* species in contrast to higher RBV/TV values toward the midline of the hand in Mc2 and Mc5 of *Gorilla*, consistent with habitual palm-back knuckle-walking. These patterns of trabecular bone distribution and structure reflect different behavioural signals that could be useful for determining the behaviours of fossil hominins.

Key words: hominid; locomotion; metacarpal; trabeculae.

Introduction

Trabecular, or cancellous, bone has been experimentally shown to remodel (Cowin, 1986; Frost, 1987) in response to loading across a range of phylogenetically disparate taxa (Biewener et al. 1996; Pontzer et al. 2006; Barak et al. 2011). Therefore, trabecular architecture can provide additional information about how a bone was loaded during life, compared with external morphology alone (Ruff & Runestad, 1992; Tsegai et al. 2013). The term 'remodelling' is used here rather than 'modelling', as it occurs throughout life and is therefore key to a bone's 'ability to function in a changing mechanical environment' (Martin et al. 1998, p. 96; see Allen & Burr, 2014). Trabeculae preserved in fossil hominins have been used to infer habitual loading and reconstruct both locomotor (DeSilva & Devlin, 2012; Barak et al. 2013a; Su et al. 2013; Zeininger et al. 2016; Ryan et al. 2018) and manipulative (Skinner et al. 2015a; Stephens et al. 2018) behaviours during human evolution. These functional inferences rely on comparative analyses that associate known behaviours of extant primates with variation in trabecular architecture at particular joints (Orr, 2016).

The hand makes direct contact with the substrate during non-human primate locomotion, and therefore its trabecular structure may provide a clearer functional signal than skeletal elements that are further removed from substrate reaction forces, such as the humerus (Ryan & Walker, 2010; Scherf et al. 2016). Indeed, previous studies of the internal bone structure of hand bones have found substantial differences between primate species with distinct habitual locomotor modes (Lazenby et al. 2011; Zeininger et al. 2011; Tsegai et al. 2013; Matarazzo, 2015; Skinner et al. 2015a; Stephens et al. 2016; Barak et al. 2017; Chirchir et al. 2017). The majority of these studies have investigated trabecular bone structure in the third metacarpal (Mc3) head because

Correspondence
Christopher J. Dunmore, Skeletal Biology Research Centre, School of Anthropology and Conservation, University of Kent, Canterbury, UK.
E: cjd37@kent.ac.uk

Accepted for publication *22 January 2019*
Article published online *17 May 2019*

the central ray is buffered from medio-lateral forces, is consistently involved in weight-bearing during locomotion, and often experiences peak reaction forces in ape locomotion (Zeininger et al. 2011; Tsegai et al. 2013; Matarazzo, 2015; Barak et al. 2017; Chirchir et al. 2017).

Different methodological approaches to the analysis of trabecular structure in the primate Mc3 head have yielded varied results. Tsegai et al. (2013) applied a whole-epiphysis approach and found that African apes had higher trabecular bone volume fraction (BV/TV) and degree of anisotropy (DA) compared with suspensory hominoids, especially in the dorsal region of the Mc3 head, consistent with an extended metacarpophalangeal (McP) joint during knuckle-walking. Suspensory orangutans and hylobatids were found to have more isotropic trabeculae and lower overall BV/TV that was highest in the palmar aspect of the Mc3, consistent with flexed-finger arboreal grips. Using fewer volumes of interest (VOI) Chirchir et al. (2017) found that there were no significant differences in DA across a sample of chimpanzees, orangutans, baboons and humans, but that BV/TV was significantly higher in distal and palmar portions of the Mc3 head in orangutans and, to a lesser extent in humans, consistent with flexed-finger grips used during arboreal locomotion and manipulation, respectively. In contrast, Barak et al. (2017), using a similar method, found the dorsal VOI in both chimpanzees and humans had significantly lower BV/TV and DA than the distal or palmar VOIs. Despite these conflicting results, these studies uniformly found that humans possessed significantly less BV/TV throughout the Mc3 head relative to other primate species (Tsegai et al. 2013; Barak et al. 2017; Chirchir et al. 2017). This finding is consistent with other skeletal elements (Chirchir et al. 2015; Ryan & Shaw, 2015) and may reflect, at least in part, lower loading of the hand during manipulation compared with that of locomotion (Tsegai et al. 2013), or sedentism in recent human populations, or both (Ryan & Shaw, 2015).

Although the whole-epiphysis approach has found a relationship between variation in metacarpal trabecular structure and hand use (Tsegai et al. 2013), this approach has been limited to comparisons of average trabecular parameters (Tsegai et al. 2013; Skinner et al. 2015a; Stephens et al. 2016) or sections thereof (Georgiou et al. 2018). Recently some researchers have called for (Chirchir et al. 2017), or developed (Sylvester & Terhune, 2017), new methods that can better quantify and statistically compare trabecular structure across different individuals and species. Here, we build on this previous work by analysing trabecular structure across all of the non-pollical metacarpal heads (Mc2-Mc5) and applying a geometric morphometric, statistical mapping method to trabecular bone data produced by the whole-epiphysis approach. We compare relative trabecular bone volume fraction (RBV/TV) and degree of anisotropy (DA) between Mc2-5 both within and across the following species: bonobos (*Pan paniscus*), chimpanzees (*Pan troglodytes*), gorillas (*Gorilla gorilla gorilla*) and orangutans (*Pongo abelii* and *Pongo pygmaeus*). RBV/TV values are BV/TV values divided by the average BV/TV of each metacarpal head (see Materials and methods).This approach allows for the quantification of trabecular architecture in a heuristic sample, less affected by issues of sub-sampling of a continuous structure, to infer differences in habitual hand loading and posture associated with hominid locomotor modes.

Hand use and locomotion

Hand postures vary greatly during different types of arboreal and terrestrial locomotion in apes (Hunt et al. 1996; Schmitt et al. 2016). However, detailed studies of hominid hand postures in the wild (Hunt, 1991; Neufuss et al. 2017; Thompson et al. 2018) and captive settings (Wunderlich & Jungers, 2009; Matarazzo, 2013a,b; Samuel et al. 2018) can inform predictions of frequent McP joint positions and loading across the hand in different species. Although frequent McP joint postures may only reflect part of a large and varied locomotor repertoire, previous research suggests (Tsegai et al. 2013; Barak et al. 2017; Chirchir et al. 2017) that subchondral trabecular patterns of the metacarpal head can be statistically discerned among species with different locomotor modes.

Pongo

Pongo pygmeaus and *P. abelii* are primarily arboreal, engaging in suspensory locomotion to move through the canopy via tree branches and lianas (Cant, 1987; Sugardjito & Cant, 1994; Thorpe & Crompton, 2005). Specifically, researchers have emphasised the use of multiple supports and quadrumanous orthograde locomotion in *Pongo* (Thorpe & Crompton, 2006; Manduell et al. 2011), though specific hand grips have not been reported in detail (Thorpe & Crompton, 2005). However, during suspension, orangutans are thought to employ a hook grip, in which the proximal phalanges align with the proximo-distal axis of the metacarpal, such that the distal McP joint is thought to be loaded in tension (Sarmiento, 1988; Rose, 1988; Schmitt et al. 2016; Fig. 1A). Similarly a double-locked grip, in which all joints of the ray, including the McP, are greatly flexed around a small substrate, is also adopted in orangutan locomotion (Napier, 1960; Rose, 1988; Fig. 1B).

The McP joints in *Pongo* possess a limited degree of possible hyper-extension at 19 degrees (Susman, 1979; Rose, 1988). Mc2-4 are also dorso-palmarly thicker at the diaphysis, and all the non-pollical metacarpal heads possess palmarly wide articular heads suggestive of habitual McP flexion (Susman, 1979). As the fourth proximal phalanx may often equal or exceed the length of the third phalanx in orangutans (40%; Susman, 1979), Rose (1988) has argued that the fourth ray is more in line with the second and third rays, which would be advantageous for both hook and double-locked grips in which rays 2–5 are typically all engaged. Although body size in *Pongo* is sexually

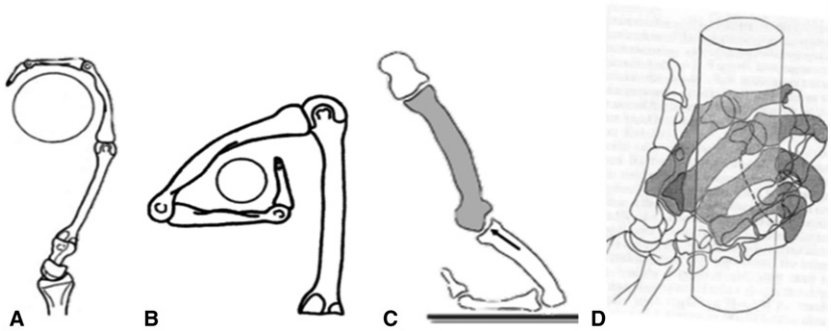

Fig. 1 Diagrammatic representations of the metacarpophalangeal postures during (A) a hook grip, (B) a 'double-locked' grip, (C) knuckle-walking and (D) a diagonal power grip. Images are adapted from Lewis (1977), Rose (1988) and Tsegai et al. (2013).

dimorphic (Rodman, 1984) and there is some evidence for differential locomotion between the sexes (Sugardjito & van Hooff, 1986), further work has found these differences to be relatively slight (Thorpe & Crompton, 2005). Therefore, we do not expect habitual prehensile postures to differ between male and female *Pongo*.

Gorilla

The most frequent locomotor mode of *Gorilla* is terrestrial knuckle-walking (Inouye, 1994; Doran, 1996; Remis, 1998); however, they can vary substantially in their degree of arboreality based on the species, sex and local ecology (Doran, 1996; Remis, 1998; Neufuss et al. 2017). The western lowland gorilla (*Gorilla gorilla gorilla*) is reported to spend probably at least 20% of its time in trees (Tuttle & Watts, 1985; Remis, 1998). During knuckle-walking, the McP joint is hyper-extended to place the arm above the weight-bearing intermediate phalanges (Tuttle, 1969; Matarazzo, 2013a,b; Fig. 1C). *Gorilla* usually uses a 'palm-back' hand posture during knuckle-walking, which places the McP orthogonal to the direction of travel while consistently loading rays 2–5, which differs from the more variable hand postures, as well as digit loading, found in *Pan* and probably reflects the relatively longer fifth digit of *Gorilla* (Tuttle, 1969; Susman, 1979; Inouye, 1992, 1994; Wunderlich & Jungers, 2009; Matarazzo, 2013a,b; but see Thompson et al. 2018). In a study of digit pressures during knuckle-walking in captive gorilla, Matarazzo (2013a,b) found that the fifth digit always touches down first, with the weight moving radially until the second (61%) or third (39%) digit lift-offs. Peak pressures were significantly lower on the fifth digit and highest on the third, but overall gorillas maintained a more even distribution of pressure across rays 2–5 than that of captive chimpanzees.

Compared with terrestrial knuckle-walking, far less is known about hand postures used by gorillas during arboreal locomotion. In captivity, *Gorilla* is described as using a power grip with little McP flexion when vertically climbing large-diameter substrates (Sarmiento, 1994). Neufuss et al. (2017) also described a similar type of power grip using all five digits and the palm-in of wild mountain gorillas (*Gorilla beringei*) when climbing larger substrates. However, when climbing medium-sized substrates (6–10 cm diameter), mountain gorillas used a diagonal power grip, in which the substrate lies diagonally across the fingers and palm, with an extremely ulnarly deviated wrist posture (Neufuss et al. 2017; Fig. 1D). In this diagonal power grip, weight appeared to be frequently borne by digits 2–4, while the fifth McP joint was unable to flex to the same extent due to the irregular shape of some substrates. Although similar data on arboreal hand postures are not available for *G. gorilla*, we assume that during arboreal locomotion, the *G. gorilla* McP joints are moderately flexed, and that this flexion increases as the substrate diameter decreases, with potentially less flexion at the fifth McP joint. However, this arboreal McP posture is likely less frequent than that associated with knuckle-walking in *Gorilla*. Indeed, although female individuals are more arboreal than larger males in *Gorilla* (Remis, 1995), the primary locomotor mode for both sexes is knuckle-walking (Tuttle & Watts, 1985; Remis, 1995; Crompton et al. 2010).

Pan troglodytes

Generally *P. troglodytes* is thought to be more arboreal than *Gorilla* (Remis, 1995; Doran, 1996; Thorpe & Crompton, 2006), though this may be the result of comparisons with mountain gorillas that are better habituated to humans compared with their more arboreal lowland counterparts (Doran, 1997; Hunt, 2004, Neufuss et al. 2017). There is a large degree of variation in the chimpanzee locomotor repertoire depending on the local ecology (Doran & Hunt, 1996; Carlson et al. 2006). *Pan troglodytes verus*, the subspecies that comprises the majority of the current sample, engages in knuckle-walking, both arboreal and terrestrial, in ~ 85% of their locomotion and spends more time in the trees than *P. troglodytes schweinfurthii* does (Doran & Hunt, 1996; Carlson et al. 2006). Compared with *Gorilla, P. troglodytes* uses more varied hand postures during knuckle-walking (Tuttle, 1969; Inouye, 1994; Matarazzo, 2013a,b). Chimpanzees have been thought to primarily load digits 3 and 4 during knuckle-walking (Tuttle, 1969; Tuttle & Basmajian, 1978). Inouye (1994) found that during captive terrestrial knuckle-walking, larger chimpanzees used their second digit significantly less often compared with gorillas of equivalent size, and both chimpanzees and bonobos generally used their fifth digit significantly less often than

gorillas did. Pressure studies also found that the fifth digit of chimpanzees did not touch-down in 20% of knuckle-walking steps and that this digit experienced significantly less load than the other digits when it was used (Wunderlich & Jungers, 2009; Matarazzo, 2013a,b). Further, *P. troglodytes* uses both 'palm-back' (~ 40%) and 'palm-in' (~ 60%) postures, compared with a more consistent use of mainly 'palm-back' (~ 86%) knuckle-walking postures in *Gorilla* (Wunderlich & Jungers, 2009; Matarazzo, 2013a,b). During 'palm-in' knuckle-walking, the intermediate phalanges roll radially in the direction of travel and the second or third digit usually experiences the highest pressures (Wunderlich & Jungers, 2009; Matarazzo, 2013a,b). In 'palm-back' knuckle-walking the third digit is typically placed in front the others and usually is the last to touch off, which may be related to the fact that the third ray may be relatively longer in chimpanzees than in gorillas (Matarazzo, 2013a,b). Compared with *Gorilla*, the peak pressures experienced by digits 2–4 are more variable in chimpanzees (Wunderlich & Jungers, 2009; Matarazzo, 2013a,b).

P. troglodytes verus most often uses climbing and scrambling locomotion in trees (60–77%; Doran, 1992, 1993). Chimpanzees are described as using power grips, diagonal power grips and hook grips during arboreal locomotion, all of which typically involve some degree of flexion at the McP joint (Napier, 1960; Hunt, 1991; Marzke et al. 1992; Alexander, 1994; Marzke & Wullstein, 1996). Climbing often encompasses vertical climbing and clambering in naturalistic studies. Hunt (1991) has emphasised the role of vertical climbing in wild *P. troglodytes* and although the grips employed tend to be ulnarly deviated at the wrist, they are dependent on substrate diameter. Neufuss et al. (2017) also found that chimpanzees used both power grips and diagonal power grips, but with a less ulnarly deviated wrist than in *Gorilla*. A diagonal power grip involves greater flexion of the more ulnar rays and in some cases, flexion at the fifth carpometacarpal joint, which may likely be associated with wrist adduction (Marzke & Wullstein, 1996; Fig. 1D). Therefore, the locomotor hand postures of *P. troglodytes* may be characterised as primarily those of knuckle-walking but with a more frequent arboreal grasping component than in *Gorilla*. Given the lower sexual dimorphism relative to *Gorilla* and *Pongo* (Doran, 1996), there may be less variation in grasping postures in this species.

Pan paniscus

While bonobos have a relatively similar locomotor repertoire to chimpanzees, they are thought to be more arboreal (Alison & Badrian, 1977; Susman et al. 1980; Susman, 1984) and have been shown to use significantly more palmigrady in the trees (Doran, 1993; Doran & Hunt, 1996; Crompton et al. 2010). Though the former claim may be an artefact of incomplete habituation of the individuals in these studies and more data are needed (Hunt, 2016), the relatively longer and heavier lower limbs of this species make for more generalised anatomy than that of chimpanzees (Zihlman, 1984; D'Août et al. 2004). During terrestrial knuckle-walking bonobos use the fifth digit even less than chimpanzees and Mc5 is shorter than the rest of the metacarpals in bonobos (Inouye, 1994). In a pressure study of arboreal locomotion, Samuel et al. (2018) found that captive bonobos used 'palm-back' (64%) or 'palm-in' (36%) knuckle-walking hand postures and that peak pressure was experienced by or around the third digit. However, unlike chimpanzees (Wunderlich & Jungers, 2009), they did not roll radially across their digits and the fifth digit always made contact with the substrate (Samuel et al. 2018). During vertical climbing and suspensory postures, bonobos used flexed-finger power grips similar to those described in other great apes and, again, peak pressure was experienced by or around the third digit (Samuel et al. 2018). In summary, the hand postures used during locomotion in *P. paniscus* can be characterised as similar to those of *P. troglodytes*, including a relatively low level of sexual dimorphism compared with other great apes (Doran, 1996), although more frequent palmigrady and arboreal grasping differentiate this species from *P. troglodytes*.

Predictions

Based on the summary above, we predict RBV/TV and DA in *Pongo* will be significantly higher in the disto-palmar region of the metacarpal heads compared with other hominids and no significant inter-ray differences in both measures due to the more consistent recruitment of rays 2–5 during hook and double-locked grasping. In *Gorilla* we predict a significantly higher dorsal distribution of RBV/TV and DA in each metacarpal head compared with all other hominids, reflecting McP joints frequently loaded in a hyperextended posture during knuckle-walking. As *P. troglodytes* may be more arboreal and uses more variable knuckle-walking postures, we predict this species will have significantly lower dorsal RBV/TV and DA, with more significant differences across rays, than that of *Gorilla*. We also predict this mixture of arboreality and terrestrially in *P. troglodytes* will elicit higher dorsal RBV/TV and DA than *Pongo* but with a more homogeneous distribution within each metacarpal head. We predict *P. paniscus* trabecular patterning will be similar to that of *P. troglodytes*, and thus possess significantly higher palmar distribution of RBV/TV and DA compared with *Gorilla* and a more dorsal distribution of these measures than seen in *Pongo.* However, we also expect *P. paniscus* to have lower DA and further homogenised distribution of RBV/TV compared with *P. troglodytes* due to more frequent use of palmigrady and arboreal grips.

Materials and methods

Subchondral trabecular bone was analysed in the metacarpus of *P. paniscus* (n = 10), *P. troglodytes* (n = 13), *G. gorilla gorilla* (n = 12), *Pongo* sp. indet. (n = 1), *P. pygmaeus* (n = 7) and *P. abelii* (n = 3).

Metacarpi were sampled from the Royal Museum for Central Africa, Tervuren, the Max Planck Institute for Evolutionary Anthropology, Leipzig, the Powell-Cotton Museum, Birchington, Bavarian State Collection of Zoology, Munich, the Natural History Museum, Berlin, the Senckenberg Natural History Museum, Frankfurt, and the Smithsonian National Museum of Natural History, Washington, DC (Table 1). All specimens were adult, wild shot and free from external signs of pathology. Within each taxon efforts were made to ensure the samples were sex balanced with even numbers of right and left metacarpi, neither ratio was more imbalanced than 5:7 for any sample. While great ape locomotion is sexually biased (Doran, 1996) and there has been some evidence for lateralised asymmetry

Table 1 Study sample.

Taxonomy	Accession ID	Sex	Side	Institution
Gorilla gorilla gorilla	PC_MER_300	Female	Left	Powell-Cotton Museum
Gorilla gorilla gorilla	PC_MER_264	Male	Right	Powell-Cotton Museum
Gorilla gorilla gorilla	PC_MER_372	Male	Left	Powell-Cotton Museum
Gorilla gorilla gorilla	PC_MER_95	Female	Right	Powell-Cotton Museum
Gorilla gorilla gorilla	PC_MER_962	Male	Left	Powell-Cotton Museum
Gorilla gorilla gorilla	PC_CAMI_230	Male	Left	Powell-Cotton Museum
Gorilla gorilla gorilla	PC_MER_138	Female	Left	Powell-Cotton Museum
Gorilla gorilla gorilla	PC_MER_174	Male	Right	Powell-Cotton Museum
Gorilla gorilla gorilla	PC_MER_696	Female	Right	Powell-Cotton Museum
Gorilla gorilla gorilla	PC_MER_856	Female	Left	Powell-Cotton Museum
Gorilla gorilla gorilla	PC_MER_879	Male	Left	Powell-Cotton Museum
Gorilla gorilla gorilla	PC_ZVI_32	Male	Right	Powell-Cotton Museum
Pan troglodytes verus	MPITC_11789	Male	Right	Max Planck Institute for Evolutionary Anthropology
Pan troglodytes verus	MPITC_11778	Female	Right	Max Planck Institute for Evolutionary Anthropology
Pan troglodytes verus	MPITC_13439	Female	Right	Max Planck Institute for Evolutionary Anthropology
Pan troglodytes verus	MPITC_15002	Female	Left	Max Planck Institute for Evolutionary Anthropology
Pan troglodytes verus	MPITC_11800	Female	Right	Max Planck Institute for Evolutionary Anthropology
Pan troglodytes verus	MPITC_11903	Male	Left	Max Planck Institute for Evolutionary Anthropology
Pan troglodytes verus	MPITC_11781	Male	Left	Max Planck Institute for Evolutionary Anthropology
Pan troglodytes verus	MPITC_14996	Female	Left	Max Planck Institute for Evolutionary Anthropology
Pan troglodytes verus	MPITC_15012	Male	Right	Max Planck Institute for Evolutionary Anthropology
Pan troglodytes verus	MPITC_15013	Female	Right	Max Planck Institute for Evolutionary Anthropology
Pan troglodytes verus	MPITC_15014	Male	Right	Max Planck Institute for Evolutionary Anthropology
Pan troglodytes verus	MPITC_15032	Male	Left	Max Planck Institute for Evolutionary Anthropology
*Pan troglodytes**	ZSM_AP_122	Male	Right	Bavarian State Collection of Zoology
Pongo abelii	SMF_6785	Male	Right	Senckenberg Natural History Museum, Frankfurt
Pongo abelii	SMF_6779	Female	Left	Senckenberg Natural History Museum, Frankfurt
Pongo pygmaeus	ZSM_1907_0633b	Female	Right	Bavarian State Collection of Zoology
Pongo pygmaeus pygmaeus	ZSM_1907_0660	Female	Right	Bavarian State Collection of Zoology
Pongo sp.	ZSM_AP-120	Male	Left	Bavarian State Collection of Zoology
Pongo pygmaeus pygmaeus	ZSM_1907_0483	Female	Right	Bavarian State Collection of Zoology
Pongo pygmaeus pygmaeus	ZSM_1909_0801	Male	Right	Bavarian State Collection of Zoology
Pongo abelii	NMNH_267325	Male	Left	Smithsonian Institution National Museum of Natural History
Pongo pygmaeus	ZMB_6948	Female	Left	Natural History Museum, Berlin
Pongo pygmaeus	ZMB_6947	Male	Left	Natural History Museum, Berlin
Pongo pygmaeus	ZMB_87092	Female	Right	Natural History Museum, Berlin
Pan paniscus	MRAC_15293	Female	Left	Royal Museum for Central Africa, Tervuren
Pan paniscus	MRAC_15294	Male	Left	Royal Museum for Central Africa, Tervuren
Pan paniscus	MRAC_20881	Male	Left	Royal Museum for Central Africa, Tervuren
Pan paniscus	MRAC_27696	Male	Right	Royal Museum for Central Africa, Tervuren
Pan paniscus	MRAC_27698	Female	Left	Royal Museum for Central Africa, Tervuren
Pan paniscus	MRAC_29042	Female	Right	Royal Museum for Central Africa, Tervuren
Pan paniscus	MRAC_29044	Male	Right	Royal Museum for Central Africa, Tervuren
Pan paniscus	MRAC_29045	Female	Left	Royal Museum for Central Africa, Tervuren
Pan paniscus	MRAC_29052	Male	Right	Royal Museum for Central Africa, Tervuren
Pan paniscus	MRAC_29060	Female	Right	Royal Museum for Central Africa, Tervuren

*Though this specimen was marked as *Pongo* in the collection, CT-scans demonstrate it has a fused scaphoid and os centrale, and so this specimen is treated as *Pan troglodytes*.

in both the trabecular (Stephens et al. 2016) and cortical bone of hominid metacarpals (Sarringhaus et al. 2005) we argue that neither of these signals is greater than the species locomotion differences under investigation here. Further, the use of evenly mixed samples should ameliorate these effects (see Discussion).

MicroCT scanning

Specimens were scanned with BIR ACTIS 225/300 and Diondo D3 high resolution microCT scanners at the Department of Human Evolution, Max Planck Institute for Evolutionary Anthropology, Germany, as well as with the Nikon 225/XTH scanner at the Cambridge Biotomography Centre, University of Cambridge, UK. Scan parameters were 100–160 kV and 100–140 μA, using a brass or copper filter of 0.2–0.5 mm, resulting in reconstructed images with an isometric voxel size of 24–45 μm.

Image processing

MicroCT scans of each metacarpal were isolated in Avizo 6.3 (Visualization Sciences Group; Fig. 2A) and segmented using the ray casting algorithm (Scherf & Tilgner, 2009). The segmented volume images were then processed as per the whole-epiphysis method, outlined in Gross et al. (2014). Briefly, a series of filtres run in MedTool 4.2 (Dr. Pahr Ingenieurs e.U.) isolated the inner trabecular structure (Fig. 2B) by casting rays at different angles from the outer cortical shell and terminating them on contact with background, non-bone voxels. A spherical kernel, with a diameter equal to the measured average trabecular thickness in that bone, was then used to close this inner structure (Pahr & Zysset, 2009). The 3D edge of this solid inner structure defined the boundary between subchondral trabecular and cortical bone. Subsequently, a regular 3D background grid, spaced at 2.5-mm intervals, was overlaid and a spherical VOI 5 mm in diameter was centred at each vertex of the grid in which BV/TV and DA was measured (Fig. 2c). Previous studies have shown that these two variables are correlated with the mechanical properties of trabecular bone, reflect bone functional adaptation (Odgaard et al. 1997; Uchiyama et al. 1999; Pontzer et al. 2006; Barak et al. 2011; Lambers et al. 2013a,b) and that they are not strongly allometric (Doube et al. 2011; Barak et al. 2013b; Ryan & Shaw, 2013). DA was measured via the mean intercept length (MIL) method and was bounded between 0 (total isotropy) and 1 (total anisotropy) using the calculation: 1 – (lowest eigenvalue of the fabric tensor/greatest eigenvalue fabric tensor). Both trabecular values were then separately interpolated on a regular 3D tetrahedral mesh of the trabecular model (Fig. 2D), created using CGAL (www.cgal.org). The surface of the trabecular mesh was extracted using Paraview (www.paraview.org) and smoothed, to permit landmark sliding (see below), in Meshlab (Cignoni et al. 2008) via a screened Poisson surface reconstruction filter (Kazhdan & Hoppe, 2013; Fig. 2E). For left-hand bones this surface mesh was mirrored in Meshlab so that it was oriented in the same was as those from right hands to permit homologous functional comparisons.

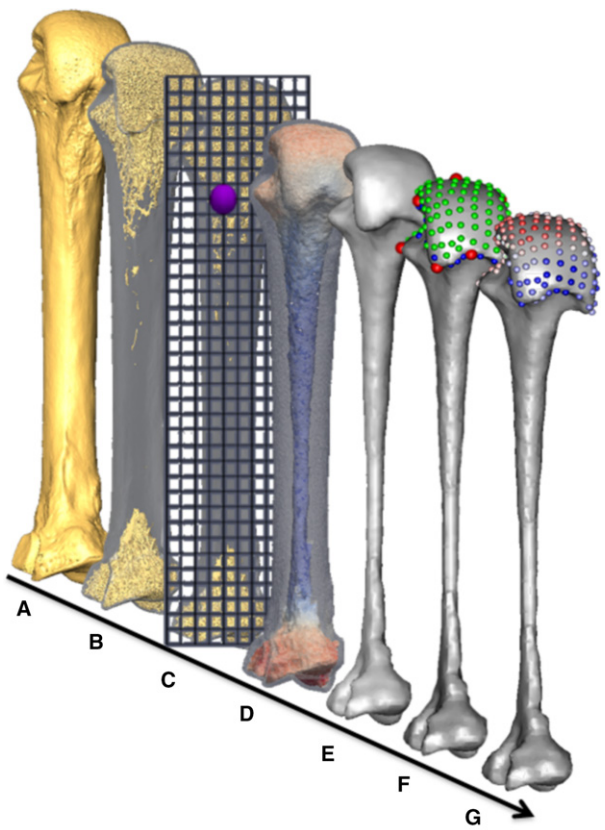

Fig. 2 Methodological stages of metacarpal trabecular analysis, shown in a third metacarpal as an example: (A) isosurface model, (B) segmented trabecular structure inside cortical shell, (C) diagram of the background grid and one of the VOIs at a vertex (purple), (D) volume mesh coloured by BV/TV (0–45%), (E) smoothed trabecular surface mesh, (F) surface landmarks (anatomical = red, semi-sliding landmarks on curves = blue and on surfaces = green), (G) RBV/TV interpolated to each surface landmark.

Geometric morphometric mapping

The whole-epiphysis method maps the entire volumetric trabecular model, but we focused our analysis on the trabecular bone beneath the articular surface of the metacarpal heads because external loads necessarily pass through these subchondral trabeculae before they can be transmitted to any other part of the trabecular structure (Zhou et al. 2014; Sylvester & Terhune, 2017). We employed a 3D geometric morphometric (GM) approach (Gunz & Mitteroecker, 2013) to trabecular analysis similar to that of Sylvester & Terhune (2017) and tested for significant differences between groups using homologous landmarks on the subchondral trabecular surface.

Anatomical landmark definitions

Many landmarks have been identified on the non-pollical metacarpals for morphometric studies (Susman, 1979; Inouye, 1992; Drapeau, 2015), but there have been relatively few studies that have applied GM methods to the primate metacarpus, and these have focused on the Mc1 base (Niewoehner, 2005; Marchi et al. 2017). Metatarsals are developmental serial homologues of metacarpals (Rolian et al. 2010) and a relatively recent study captured their shape variation using a patch of 3D landmarks (Fernández et al. 2015). A recent study of Mc3 head shape used most of the same landmarks that bordered on this metatarsal patch, at the homologous metacarpal locations (Rein, 2018). Based on these studies, the location and type (Bookstein, 1991) of anatomical landmarks used here are given in Table 2. Although the internal trabecular subchondral surface is landmarked, cortical bone is very thin at the

Table 2 Anatomical landmark definitions, types (Bookstein, 1991) and their provenance. Each article describes the landmark, using it as the terminus of a linear measure or directly for GM analysis.

Number	Type	Description	Provenance
1	Type II	Most proximal point under the ulnar palmar epicondyle (anterior eminence)	Yeh & Wolf (1977), Fernández et al. (2015), Rein (2018)
2	Type III	The point of maximum curvature on the inter-epicondylar ridge between points 1 and 3	Drapeau (2015), Fernández et al. (2015), Rein (2018)
3	Type II	Most proximal point under the radial palmar epicondyle (anterior eminence)	Yeh & Wolf (1977), Fernández et al. (2015), Rein (2018)
4	Type III	Point of maximum curvature on the radial ridge separating the articular surface from the radial lateral sulcus	Yeh & Wolf (1977), Fernández et al. (2015), Rein (2018)
5	Type II	Most radially projecting point under the ulnar dorsal tubercle	Yeh & Wolf (1977), Susman (1979), Inouye (1992), Fernández et al. (2015), Rein (2018)
6	Type III	Mid-point between the posterior tubercles on the intertubercular ridge, underlying the dorsal ridge if present.	Yeh & Wolf (1977), Fernández et al. (2015)
7	Type II	Most ulnarly projecting point under the ulnar dorsal tubercle	Yeh & Wolf (1977), Susman (1979), Inouye (1992), Fernández et al. (2015), Rein (2018)
8	Type III	Point of maximum curvature on the ulnar ridge separating the articular surface from the ulnar lateral sulcus	Yeh & Wolf (1977), Fernández et al. (2015), Rein (2018)
9	Type II	Most distally projecting point on the subchondral surface	Fernández et al. (2015); Susman (1979), Inouye (1992), Rein (2018)

metacarpal head in hominids (Tsegai et al. 2017) and so the correspondence between these surfaces is generally high. Though the articular surface may not cover the same area in all species studied, the same landmarks are used for comparison as they are present on all metacarpal heads studied.

Repeatability

Landmarks were manually placed in Checkpoint (Stratovan Corporation, Davis, CA, USA) and repeated 10 times on three randomly selected specimens from each species over several days. A different ray was used from each species to ensure landmarks were repeatable across elements following Fernández et al. (2015). The landmarks were then aligned using Procrustes superimposition in the Morpho package in R v3.3.0 (R Core Development Team, 2016; Schlager, 2017). Landmark configurations were then plotted in the first two principal components (PC) of shape space. Landmarks were considered stable if repeated measures were more clustered than those of different individuals. Significant pair-wise permutational manovas conducted on PC1 and PC2 scores demonstrated that group means of the three individuals and their repeats, are significantly different in each case and that variance in landmark placement is significantly less than that between specimens (Supporting Information Fig. S1).

Geometric morphometric procedure

To create the landmark template, a random specimen was selected and eight curves were defined at the margins of the sub-articular surface, in Checkpoint, each bordered by anatomical landmarks as recommended by Gunz et al. (2005). Three sliding semi-landmarks were placed on each of these curves and an additional 140 were equally distributed over the sub-articular surface in Avizo 6.3 (Visualization Sciences Group, Germany) to create a 173-landmark template. The anatomical landmarks were subsequently placed on every specimen and the landmark template (Fig. 2F) then projected onto each of the 183 other metacarpal heads and relaxed onto the surface of each metacarpal using the Morpho package in R (Schlager, 2017) by minimizing bending energy. This package was then used to slide the semi-landmarks along their respective curves and over the surface by minimizing Procrustes distances. This slid template is plotted on an individual Mc3 from each species to provide a sense of the shape variation present (Supporting Information Fig. S6).

Data mapping

Using a custom Python script plugin for Paraview (www.paraview.org) the non-smoothed surface mesh triangles inherited trabecular values from their originating tetrahedra. The Python module SciPy (Jones et al. 2001) was then used in medtool 4.2 (Dr. Pahr Ingenieurs e.U.) to interpolate the trabecular values to the nearest landmark; this was done separately for BV/TV and DA. Interpolating these trabecular values from the outer tetrahedra of the trabecular model is analogous to using spherical VOIs, 1 mm in diameter, centred 0.5 mm beneath an inner trabecular surface landmark. Finally, the geomorph package (Adams et al. 2017) in R was used to perform a generalised Procrustes procedure, resulting in 184 sets of 173 homologous landmarks each with two associated trabecular values (Fig. 2G).

Relative trabecular volume

We employ a relative measure of bone volume fraction (RBV/TV), in which the raw BV/TV value of each landmark is divided by the mean of all landmark BV/TV values on that metacarpal head. Thus RBV/TV values ~ 1 indicate landmarks close to the average BV/TV of that Mc head, while values above or below 1 indicate a deviation from this average at these landmarks. This relative measure was preferred because, while BV/TV can vary systemically across extant hominid species (Tsegai et al. 2018) and may show considerable intraspecific variation, the relative patterns of trabecular architecture appear to preserve a functional signal superimposed on this variation (Saers

et al. 2016). RBV/TV measures the position of the greatest subchondral trabecular bone of a given Mc head rather the absolute volume of bone and therefore is argued to reflect the habitually loaded joint positions of extant hominids while controlling, at least in part, for intra-species and systemic inter-species differences. Species average absolute BV/TV landmark values are depicted for comparison with RBV/TV values in Fig. 3 (see Supporting information).

Statistical analysis

We employ a 'mass-univariate' approach as advocated by Friston et al. (1995) similar to that used to statistically analyse cortical bone in ape metacarpals (Tsegai et al. 2017). Specifically, the trabecular values between species and rays at each landmark are independently analysed using univariate statistics. Inter-ray comparisons do not include comparisons between rays two and four or between rays three and five as they are not biologically contiguous and thus are less informative when prehensile hand postures are considered. However, comparisons of rays two and five are included to test for significant differences between the most ulnar and radial aspects of the metacarpus. Shapiro-Wilk tests found a non-normal distribution of data at one or more landmarks in one or both groups in every pair-wise, inter-ray and interspecific, comparison. To maintain consistent comparisons, a non-parametric Kruskal–Wallis test was applied at each landmark and a post-hoc test was used to test for pair-wise differences if the omnibus test was significant. Dunn's test was chosen as it uses the pooled variance of the Kruskal–Wallis tests and so is conservative. The level of significance was set at $P < 0.05$ subsequent to a Bonferroni correction in each case. This univariate approach means that homologous landmark values are compared across groups rather than with spatially correlated neighbouring landmarks. *Z*-scores were used to determine the polarity, as well as the effect size, of significant differences between groups. These *Z*-scores were transformed into absolute, rather than signed, values and summarised for significant landmark differences, in both interspecific and inter-ray pair-wise comparisons (Supporting Information Tables S1 and S2). Resulting plots of significant univariate differences map regional differences between species and rays but were only considered meaningful if they were found at nine contiguous landmarks, as this represents just over 5% of the sub-articular surface, in order to further ameliorate any Type I error. Despite the fact this univariate method can identify where regions of significant difference lie, it can be susceptible to Type I error and so to provide a multivariate corollary to this approach, a principle components analysis (PCA) of trabecular values, using landmarks as individual variables, was also run for all comparisons. Subsequent omnibus and pair-wise one-way permutational MANOVAs were run with a Bonferroni correction, using the VEGAN package (Oksanen et al. 2018) in R v3.3.0 (R Core Development Team 2016), on the principal component scores of these PCAs to test for significant overall, rather than regional, differences in trabecular patterns.

Results

Univariate landmark comparisons

Pongo

RBV/TV was highest in the palmar aspect of all metacarpal heads in *Pongo* (Fig. 3). The significant differences among the rays included those between Mc2 and Mc5, each of which had a small patch of significantly higher RBV/TV at the ulnar and radial aspects of the metacarpal head, respectively (Fig. 5). Mc3 also had a patch of significantly higher RBV/TV at radio-palmar landmarks relative to Mc2. Interspecifically, *Pongo* RBV/TV was significantly higher at landmarks in the palmar region of the metacarpal heads compared with *P. troglodytes* and especially *Gorilla* (Fig. 7). Compared with *P. paniscus, Pongo* was again significantly higher at more palmar landmarks in Mc4 and Mc5 but there were fewer significantly higher landmarks in Mc3 and almost none in the Mc2 comparison.

Pongo had high DA values throughout the sub-articular metacarpal heads with few significant differences between

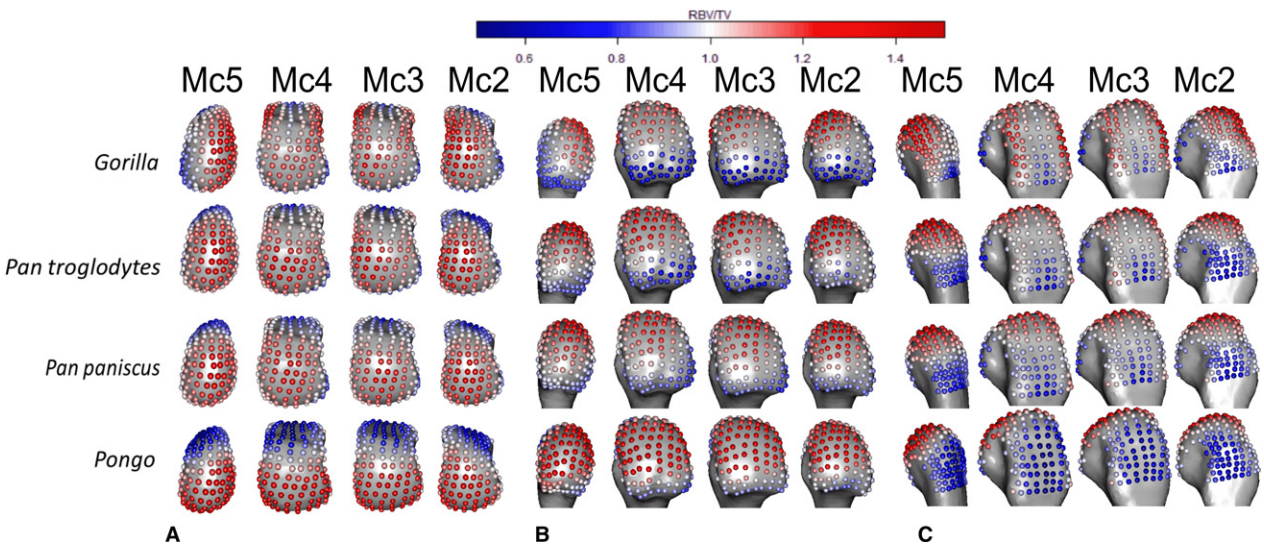

Fig. 3 Species average RBV/TV, mapped to average models of each Mc head in (A) distal, (B) palmar and (C) dorsal views. RBV/TV values around one (white) indicate landmarks close to the average BV/TV of that Mc head, while values above (red) or below one (blue) indicate a deviation from this average at these landmarks.

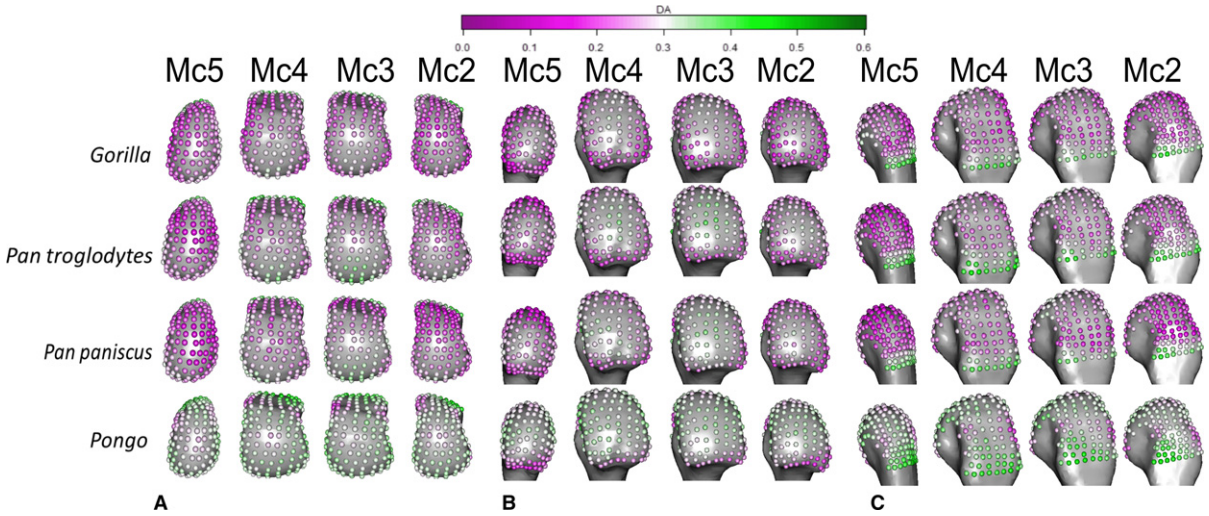

Fig. 4 Species average DA mapped to average models of each Mc head in (A) distal, (B) palmar and (C) dorsal views.

rays (Figs 4, 6 and S3). Interspecifically, *Pongo* DA was significantly greater than that of *Gorilla* in all metacarpal heads except for the central disto-palmar aspects of Mc3-4 and radio-palmar aspects of Mc5. *Pongo* had significantly higher DA on the disto-dorsal aspects of Mc2 and Mc5 relative to both *P. troglodytes* and *P. paniscus*. *Pongo* also had higher DA at landmarks situated on the dorsal aspects of Mc 3 and 4 relative to *P. paniscus* (Fig. 8).

Gorilla

The highest RBV/TV values in *Gorilla* were concentrated in the disto-dorsal portion of each metacarpal head extending dorsally on the medio-lateral edges of Mc3 and 4 but toward the midline of the hand in the Mc2 and Mc5 heads (Fig. 3). This latter pattern was clear in the inter-ray comparison, with significantly greater RBV/TV found at the radial aspect of Mc5 relative to Mc2 and Mc4 as well as on the ulnar aspect of these rays relative to Mc5 (Fig. 5). Interspecifically, *Gorilla* was significantly higher in RBV/TV dorsally compared with *Pongo*, though the radio-palmar aspect of Mc5 was not significantly different between these groups. Compared with *Pan*, *Gorilla* generally had significantly higher RBV/TV dorsally but this was restricted to the medio-lateral edges of each metacarpal head in the regional comparison (Fig. 7). Specifically, *Gorilla* had significantly higher RBV/TV than *Pan* species on the radio-dorsal aspect of Mc5 and both medio-lateral edges of Mc4, as well as the ulno-dorsal aspect of Mc2, though this is extended across the dorsal aspect in the *P. troglodytes* comparison. The Mc3 of *Gorilla* also had significantly higher RBV/TV than *P. paniscus* at landmarks on its dorso-ulnar aspect but was not significantly different from *P. troglodytes* in any region. *Gorilla* had less significant regional differences with *P. troglodytes* than with *P. paniscus* in RBV/TV.

Gorilla had low DA throughout the subchondral metacarpal head trabeculae with slightly higher values distally on Mc3 and Mc4, though only the ulnar-distal aspect of Mc3 had values that were significantly larger than Mc2 (Figs 4 and 6). Mc5 had significantly higher DA on its radial side relative to Mc2 (Fig. 6). *Gorilla* was not significantly higher in DA than were other taxa, apart from the radial border of the distal Mc5 head compared with *Pan paniscus* (Fig. 8).

Pan troglodytes

P. troglodytes had disto-dorsally higher RBV/TV values in the subchondral trabeculae of all the metacarpal heads, though this pattern was more dorsally positioned in Mc3 and Mc4 (Fig. 3). Mc2 and Mc5 showed significantly higher RBV/TV at their most palmar extent relative to Mc3 and Mc4, respectively (Fig. 5). Interspecifically, *P. troglodytes* showed almost no significant differentiation from *P. paniscus* in RBV/TV in any ray (Fig. 7). *P. troglodytes* had significantly higher RBV/TV across the palmar extent of Mc2, and disto-palmarly on the ulnar aspect of Mc5 compared with that of *Gorilla*, and significantly higher RBV/TV dorsally than *Pongo* in each ray.

P. troglodytes generally had low DA through all of the metacarpal heads, although DA values were slighter higher in the palmar regions of Mc3 and Mc4 (Fig. 4). DA values were significantly higher in Mc4 relative to Mc5 and higher in Mc3 relative to Mc2 (Fig. 6). *P. troglodytes* showed the fewest significant differences in DA with *P. paniscus*, significantly higher DA in the palmar aspects of Mc2 and Mc3 compared with *Gorilla*, and significantly lower DA than *Pongo* throughout all the rays (Fig. 8).

Pan paniscus

Like *P. troglodytes, P. paniscus* had the highest RBV/TV values at the disto-dorsal aspect of metacarpal heads but subchondral trabeculae structure was more homogenous within and between the rays (Figs 3 and 5). Interspecifically, *P. paniscus* showed the fewest significant differences with

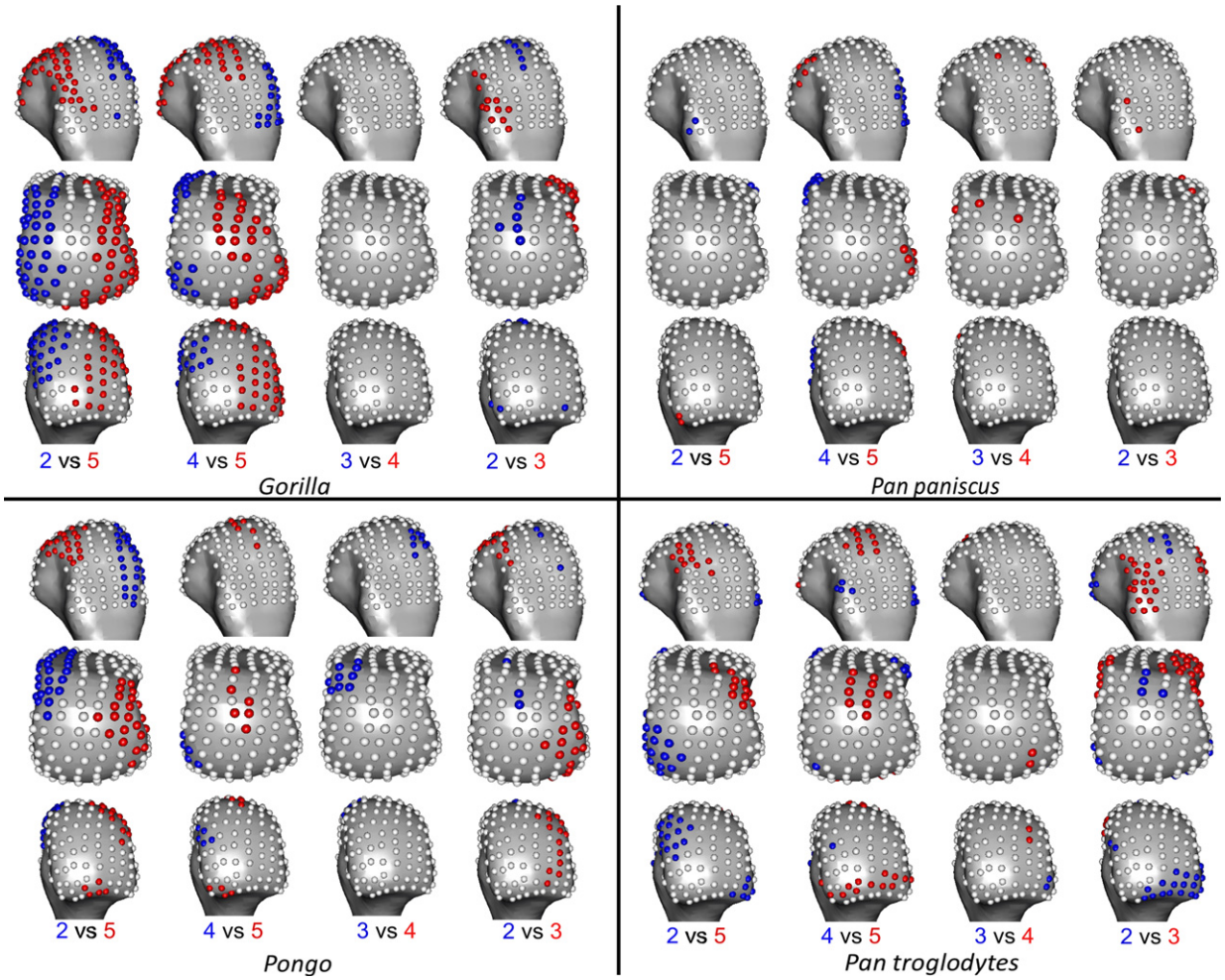

Fig. 5 Inter-ray significant differences in RBV/TV, mapped to an average right Mc3 head in each case in dorsal (top), distal (middle) and palmar (bottom) views. Where RBV/TV values at landmarks are significantly higher in one ray than the other, they are coloured as per the ray numbers in each comparison.

P. troglodytes apart from a small concentration of higher RBV/TV landmarks in the most palmar extent of Mc3 (Fig. 7). *P. paniscus* possessed significantly higher RBV/TV dorsally than *Pongo* across the rays and significantly higher palmar RBV/TV than *Gorilla* in all of the rays. This latter pattern extended distally on Mc2 and Mc5 (Figs 3 and 7).

P. paniscus had a similar DA pattern to *P. troglodytes*, with similar inter-ray significant differences and almost no significant differences between these species (Figs 4, 6 and 8). *P. paniscus* showed significantly higher DA than *Gorilla* did in landmarks across the Mc2 and Mc3 heads, in the palmar regions (Fig. 8). As with all other African apes, *P. paniscus* had significantly lower DA than *Pongo* did across the metacarpal heads, particularly in the dorsal regions.

Multivariate whole-surface comparisons

Interspecific results

Figure 9 depicts the results of the PCA on RBV/TV values, showing species differences within each metacarpal head. Within the Mc2-5 of all the taxa, the first principal component (PC1) explains 38–46% variation in RBV/TV and was driven by dorsal and palmar landmarks. PC2 in Mc2-Mc5 described 13–17% of the variation and reflected variation of values in landmarks that were distally and non-distally situated, respectively. In Mc5, PC3 described 14% of RBV/TV variation in values at radio-ulnar landmarks. Permutational MANOVA omnibus tests were run using PC1-3 in each case, as for some comparisons the PC2 and PC3 explained a similar amount of variance whereas further PCs each explained less than 10% of the variance. These omnibus tests were significant in every ray. As with the individual landmark comparisons described above, *Pongo* had significantly higher palmar RBV/TV compared with all other species, especially *Gorilla.* The overall configuration of *Gorilla* RBV/TV was significantly higher dorsally compared with all other species in Mc2-4 and radio-dorsally in Mc5 (Fig. 9, Table 3). *P. troglodytes* and *P. paniscus* were not significantly different from each other in any of the species comparisons (Table 3).

Following the limited interspecific differences in DA described above, a PCA of DA values yielded poor

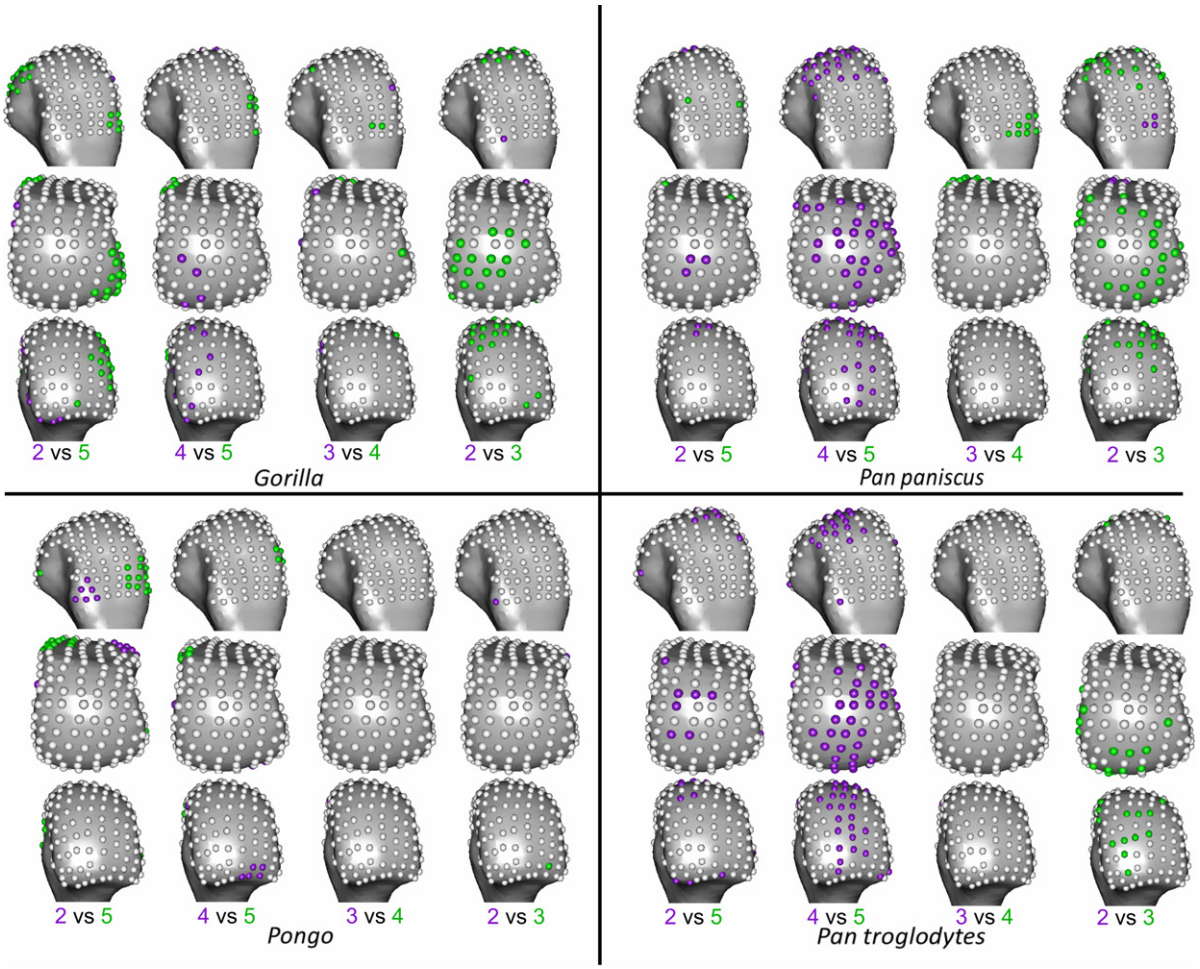

Fig. 6 Inter-ray significant differences in DA, mapped to an average right Mc3 head in each case in dorsal (top), distal (middle) and palmar (bottom) views. Where DA values at landmarks are significantly higher in one ray than the other, they are coloured as per the ray numbers in each comparison.

separation among the sampled taxa. As such, the results are depicted in the Supporting Information. PC1 in DA for each ray, across species, described 34–36% of the variation and was driven by higher values at most landmarks. PC2 described 10–14% of the variation and was driven by landmarks situated dorsally and disto-palmarly, respectively (Supporting Information Fig. S2). Although *Pongo* tended to occupy the positive end of PC1, reflecting higher DA, permutational MANOVAs on PC1-3 revealed that they were only significantly different in every ray from *Gorilla*. This result may be partially driven by the larger intra-species variation in *Pongo* DA relative to other species studied (Fig. S2, see Discussion). *Pongo* was significantly different from *P. paniscus* in Mc2, Mc3 and Mc5 as well as from *P. troglodytes* in Mc2 and Mc5, having generally higher DA (Table 3). Again, *P. paniscus* and *P. troglodytes* were not significantly different from each other at any ray, though both species were slightly, but significantly, higher in DA than *Gorilla* in most rays, *P. troglodytes* was not significantly different form *Gorilla* in DA across Mc4. Both *Pan* species had significantly lower DA than *Gorilla* in the radio-distal aspect of Mc5.

Inter-ray results

Figure 10 depicts the results of PCA of RBV/TV values, showing inter-ray differences within each species. Overall Mc head variation in RBV/TV across rays was different for each species but was generally consistent with individual landmark comparisons described above. In *Pongo,* PC1 explained 25% of the variation and was driven by dorso-palmar landmark values, whereas PC2 explained 18% of the variation and reflected radio-ulnar landmark RBV/TV. The significant omnibus result was driven solely by a Mc2 configuration that had significantly higher disto-ulnar RBV/TV than the other rays did. In *Gorilla,* PC1 reflected 27% of the variation as a result of radio-ulnar landmark values, whereas PC2 reflected 18% of the variation in RBV/TV due to distal and more dorso-palmarly located landmarks (Fig. 10). Permutational MANOVAs on PC1-3 demonstrated the *Gorilla* Mc5 had significantly higher

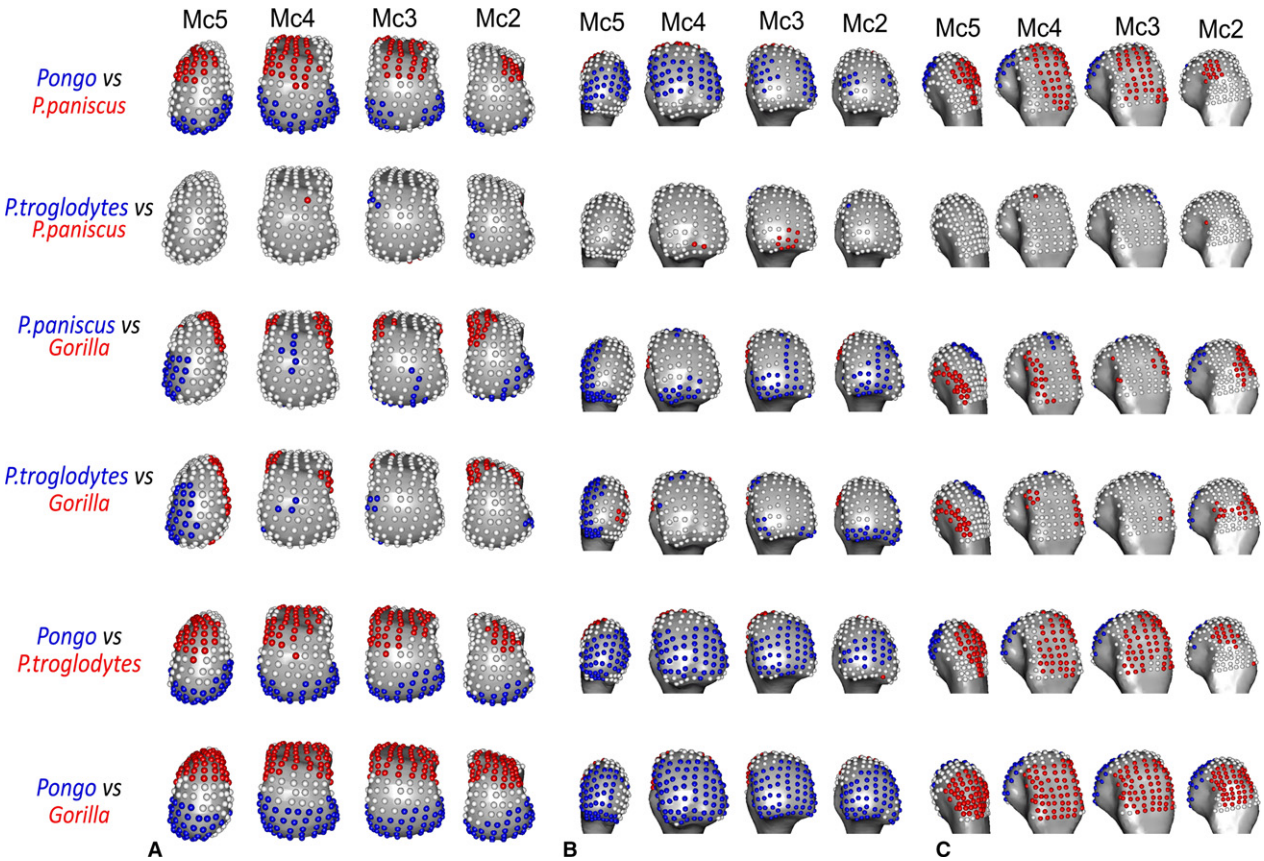

Fig. 7 Significant differences in RBV/TV between species, mapped to average models of each Mc head in (A) distal, (B) palmar and (C) dorsal views. Where RBV/TV values at landmarks are significantly higher in one species than the other, they are coloured as per the species in each comparison.

RBV/TV disto-radially relative to all other rays. *Gorilla* Mc2 had significantly higher disto-ulnar RBV/TV than the other rays, whereas Mc3 and Mc4 had significantly higher RBVTV dorsally than Mc2 and Mc5 and were not significantly different from each other (Table 3). For *P. troglodytes*, variation in overall RBV/TV was chiefly driven by dorso-palmar landmarks on PC1, which explained 32% of the variation, whereas PC2 explained 15% of the variation and reflected differences in the disto-ulnar landmarks. PC3 in *P. troglodytes* RBV/TV describes 12% of the variation and is driven by radio-ulnar landmarks (Fig. 10). *P. troglodytes* Mc2 had significantly higher RBTV/TV disto-palmarly on its ulnar aspect relative to all other rays, whereas Mc5 had significantly higher RBV/TV disto-palmarly on its ulnar aspect compared with Mc2 and Mc3. Mc3 and Mc4 were not significantly different from each other as both had higher dorsal RBV/TV, and Mc4 was not significantly different from Mc5. In *P. paniscus*, PC1 explained 36% of the variance in RBV/TV and was driven by dorso-palmar landmarks, whereas PC2 explained 24% of the variance and reflected distal and non-distal landmarks. However, no significant differences in RBV/TV were found between *P. paniscus* rays (Table 3).

Variation in DA values did not show many significant differences across the Mc heads but was broadly consistent with the individual landmark comparisons. For all species sampled, PC1 was driven by higher values at most landmarks in PC1 and explained 19–45% of the variation. PC2 described 10–16% of the variation in DA and reflected distal as opposed to non-distal landmarks in all species (Supporting Information Fig. S3). In *Pongo*, no ray was significantly different from any other in overall configuration of DA values (Table 3). In Gorilla, PC3 explained 9% of the variance and was driven by radio-ulnar landmarks. Mc5 in *Gorilla* had significantly higher DA at radial landmarks than Mc2 and Mc3 did. The *Gorilla* Mc4 had slightly, but significantly, higher DA over most landmarks relative to Mc2. Both *P. troglodytes* and *P. paniscus* had significantly lower DA at landmarks on the distal aspect of Mc5 compared with Mc3 and Mc4. *P. paniscus* alone also had significantly lower DA over most landmarks on Mc2 compared with Mc3.

Discussion

The aim of this study was to associate inferred loading during particular hand postures in great apes during locomotion with subchondral trabecular architecture across the non-pollical metacarpal heads. The results confirm and build upon previous studies of trabecular bone, most often

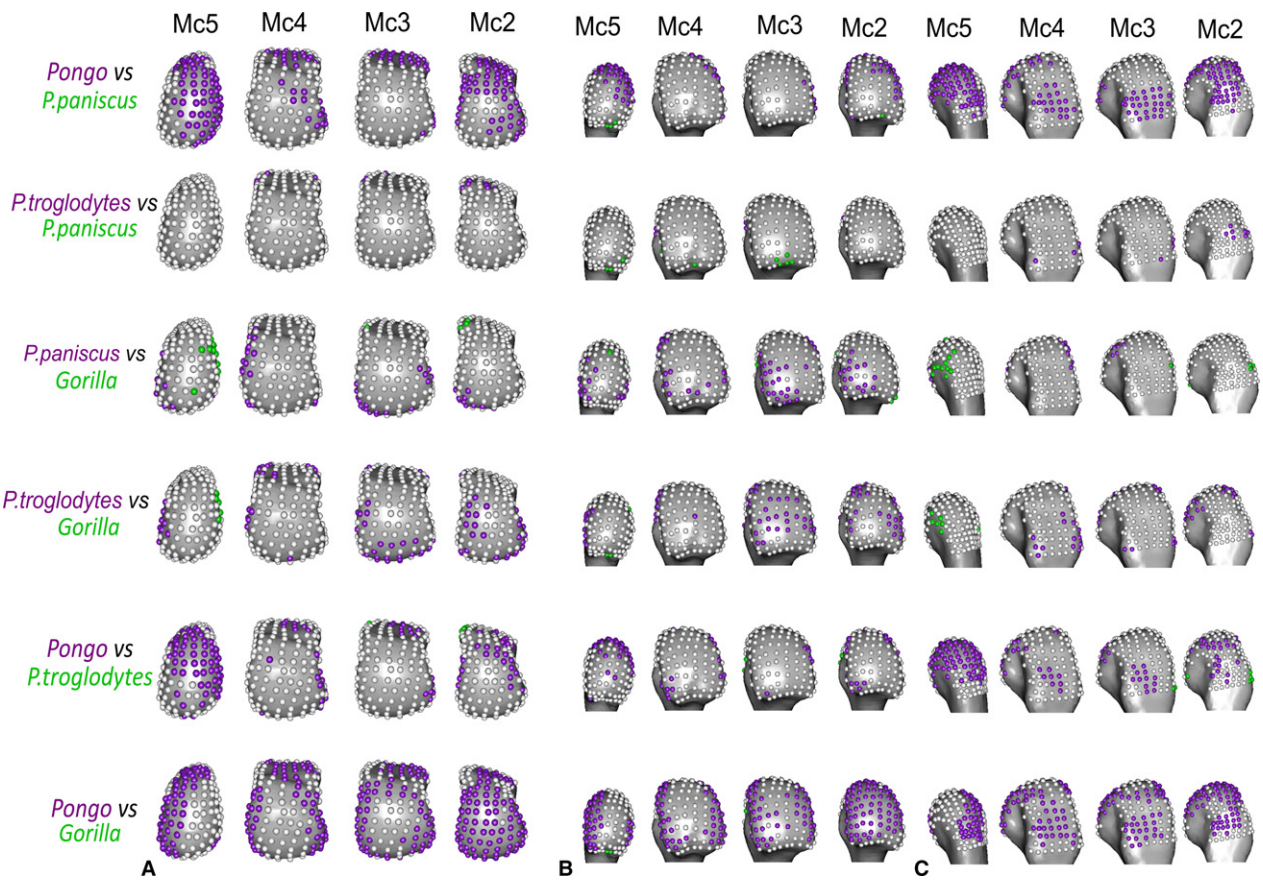

Fig. 8 Significant differences in DA between species, mapped to average models of each Mc head in (A) distal, (B) palmar and (C) dorsal views. Where DA values at landmarks are significantly higher in one species than the other, they are coloured as per the species in each comparison.

focused on only the Mc3 head (Tsegai et al. 2013; Barak et al. 2017; Chirchir et al. 2017), demonstrating not only that is this association possible but that regional trabecular patterns within metacarpal heads, both within and across species, can be statistically discerned. Further, locomotor signals within trabecular structure are not limited to the Mc3, and analysis of all non-pollical metacarpals can provide greater insight into inter-ray and interspecific differences in digit loading.

Relative trabecular bone volume fraction

Pongo

We predicted the orangutans would show significantly higher RBV/TV in the disto-palmar region of the metacarpal heads compared with other hominids and that there would be no significant differences between rays, reflecting the flexed or neutral McP joint posture of all the fingers that characterises flexed-finger power, hook and double-locked grips typically used during arboreal locomotion (Rose, 1988; Sarmiento, 1988). We found general support for these predictions. Orangutans demonstrated significantly higher RBV/TV in the disto-palmar aspect of the subchondral trabeculae in all non-pollical metacarpal heads than did all other taxa. We also found few inter-ray differences, with orangutans generally showing fewer significantly different landmarks in RBV/TV compared with gorillas and chimps (Fig. 5) and no significant difference in overall RBV/TV between adjacent rays (Table 3). The only exception to this was Mc2 of orangutans, which had significantly higher RBV/TV in the disto-dorsal region of its ulnar aspect, relative to the other rays (Figs 5 and 10). Overall, our results are consistent with previous studies using differing methodologies that also found a higher BV/TV in the disto-palmar region of the orangutan Mc3 head (Zeininger et al. 2011; Tsegai et al. 2013; Skinner et al. 2015a; Chirchir et al. 2017) and Mc5 head (Skinner et al. 2015a). It should be noted, however, that the present study sample includes five of the same Mc3 specimens and three of the Mc5 specimens used by Tsegai et al. (2013) and Skinner et al. (2015a), respectively. The generally similar pattern of RBV/TV distribution across the Mc2-5 heads is consistent with using all of the fingers during power, hook and double-lock grips to grasp arboreal substrates (Rose, 1988). The diverging pattern found in the orangutan Mc2 could reflect the relatively more extended second digit posture during a diagonal double-locked grip of very thin substrates, as pictured by Napier (1960) in captivity (Supporting Information Fig. S4).

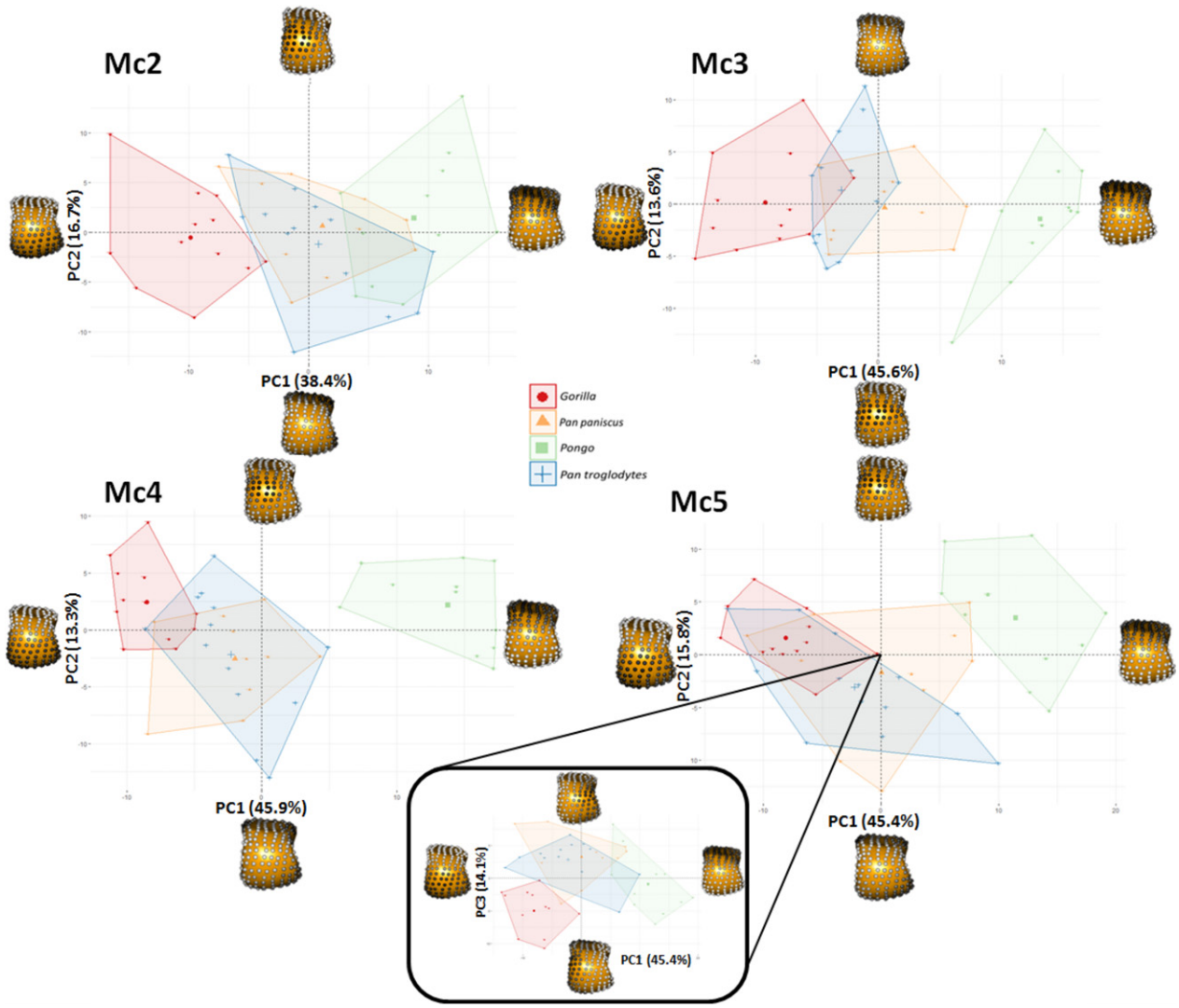

Fig. 9 RBV/TV PCA plots showing species differences within each metacarpal head. Each plot shows the first two principle components (PC) in each ray. For Mc5, PC3 is depicted with PC1 (inset), as PC2 and PC3 explain a similar amount of the variance (16 and 14%, respectively) in this case. Landmarks at each extreme of a PC are coloured in grayscale, according to their signed contribution to that PC and plotted on a Mc3 in distal view. White landmarks indicate the highest signed contribution to the PC and black the least.

However, although challenging data to collect, more behavioural studies of types and frequency of hand grips used by orangutans during arboreal locomotion are needed to substantiate this.

Gorilla

We predicted gorillas would show a significantly higher dorsal distribution of RBV/TV in each metacarpal head compared with all other hominids, reflecting McP joints loaded in a hyper-extended posture during frequent knuckle-walking; this prediction was supported. RBV/TV in the gorilla subchondral trabeculae was significantly higher dorsally than in all other species (Figs 7 and 9). This RBV/TV pattern was also found in previous studies of the Mc3 in gorillas (Tsegai et al. 2013; Skinner et al. 2015a). The present results, however, also revealed high RBV/TV along the disto-ulnar region of the Mc2 head and disto-radial region of the Mc5 head, which was not predicted, although a similar pattern was also found in the Mc5 by Skinner et al. (2015a). This pattern is present in the average male and female RBV/TV distribution (Supporting Information Fig. S5). The gorilla fifth digit is more frequently used in knuckle-walking (Inouye, 1994) and is more similar in length to the other rays compared with that of chimpanzees (Susman, 1979; Inouye, 1992), which may explain the more even distribution of knuckle-walking pressure across the digits in captive gorillas (Matarazzo, 2013a,b). As the fifth digit is often not involved in grips of thinner arboreal substrates (Neufuss et al. 2017) and this RBV/TV pattern is mirrored in the Mc2, it seems parsimonious to argue it reflects more frequent

Table 3 Permutational MANOVAS on the first three principle components between all groups.

	RBV/TV MC2	*RBV/TV MC3*	*RBV/TV MC4*	*RBV/TV MC5*		*RBV/TV Ggg*	*RBV/TV Pp*	*RBV/TV Ppy*	*RBV/TV Pt*
All	**0.0001**	**0.0001**	**0.0001**	**0.0001**	*All*	**0.0001**	0.1209	**0.0001**	**0.0001**
Ppy-Pp	**0.0066**	**0.0006**	**0.0006**	**0.0006**	*2–3*	**0.0258**	n/s	**0.0306**	**0.0012**
Pt-Pp	1.0000	0.6900	1.0000	1.0000	*3–4*	1.0000	n/s	0.9900	1.0000
Pp-Ggg	**0.0006**	**0.0006**	**0.0012**	**0.0006**	*4–5*	**0.0006**	n/s	0.0924	0.2340
Pt-Ggg	**0.0006**	**0.0120**	**0.0012**	**0.0006**	*2–5*	**0.0006**	n/s	**0.0012**	**0.0498**
Pt-Ppy	**0.0054**	**0.0006**	**0.0006**	**0.0006**	*3–5*	**0.0006**	n/s	0.1968	**0.0006**
Ppy-Ggg	**0.0006**	**0.0006**	**0.0006**	**0.0006**	*2–4*	**0.0012**	n/s	**0.0018**	**0.0084**
	DA MC2	*DA MC3*	*DA MC4*	*DA MC5*		*DA Ggg*	*DA Pp*	*DA Ppy*	*DA Pt*
All	**0.0001**	**0.0001**	**0.0001**	**0.0001**	*All*	**0.0003**	**0.0001**	0.2737	**0.0018**
Ppy-Pp	**0.0006**	**0.0222**	**0.0636**	**0.0024**	*2–3*	0.4032	**0.0264**	n/s	0.4710
Pt-Pp	0.6234	1.0000	1.0000	1.0000	*3–4*	1.0000	0.4302	n/s	1.0000
Pp-Ggg	**0.0402**	**0.0102**	**0.0378**	**0.0006**	*4–5*	0.0900	**0.0012**	n/s	**0.0162**
Pt-Ggg	**0.0180**	**0.0336**	**0.0828**	**0.0342**	*2–5*	**0.0096**	0.3318	n/s	0.3894
Pt-Ppy	**0.0054**	0.1626	0.0135	**0.0036**	*3–5*	**0.0108**	**0.0012**	n/s	**0.0036**
Ppy-Ggg	**0.0006**	**0.0006**	**0.0018**	**0.0036**	*2–4*	**0.0114**	0.0930	n/s	1.0000

Species abbreviations are: Ggg, *Gorilla;* Pt, *Pan troglodytes;* Pp, *Pan paniscus;* Ppy, *Pongo* spp. Subsequent pair-wise tests were carried out if the omnibus test was significant; otherwise pair-wise tests are marked as non-significant (N/S). All *P*-values reported are subsequent to a Bonferroni correction and are marked in bold where significant.

and less variable knuckle-walking hand postures in gorillas relative to chimpanzees and bonobos (Tuttle & Basmajian, 1978; Matarazzo, 2013a,b; Thompson et al. 2018). The Mc3 and Mc4 of gorillas also showed high RBV/TV dorsally, especially at the radio-ulnar margins (Figs 3 and 5), which is consistent with the idea that the fingers work in concert to buffer medio-lateral forces during locomotion (Chirchir et al. 2017). The medio-lateral forces generated during 'palm-back' knuckle-walking, which places the McP joints orthogonal to the direction of travel, may be considerable.

Pan troglodytes

We predicted that chimpanzees would have significantly higher dorsal RBV/TV than orangutans but lower than in gorillas, with a more homogeneous distribution of RBV/TV within each metacarpal head and more inter-ray differences, reflecting their more varied locomotor regimen. These predictions were generally supported. The disto-dorsal pattern of higher RBV/TV across the subchondral metacarpus of chimpanzees (Fig. 3) was more dorsally concentrated than in orangutans and more distally extended than in gorillas (Figs 7 and 9). This RBV/TV pattern is consistent with previous studies of chimpanzee subchondral trabecular bone (Zeininger et al. 2011) and whole-epiphyseal analyses that found a similar signal in the subchondral trabeculae of Mc3 and Mc5 (Tsegai et al. 2013; Skinner et al. 2015a). It should be noted, however, that the present study sample includes five of the same Mc3 specimens and four of the Mc5 specimens used by Tsegai et al. (2013) and Skinner et al. (2015a), respectively. In contrast to these analyses, studies using larger VOI methods have found higher BV/TV in centrally placed VOIs relative to palmar or dorsally placed VOI's in the chimpanzee Mc3 head (Barak et al. 2017; Chirchir et al. 2017). However, the use of fewer large VOIs in these studies, as opposed to the many smaller VOIs produced by the whole-epiphysis approach employed here, may exacerbate issues of VOI placement and size that have been shown to have a dramatic effect on trabecular measures in the primate Mc3 (Kivell et al. 2011).

In partial support of our prediction, we found that chimpanzees showed several significant differences in RBV/TV between the Mc heads, although there were not more differences than those found in gorillas. Specifically, RBV/TV in chimpanzees was significantly higher palmarly in Mc2 and Mc5 but higher distally in Mc3 and Mc4 (Figs 5 and 10). This pattern may reflect relatively more weight-bearing by digits 3 and 4 during knuckle-walking than in the second or fifth digit (Tuttle & Basmajian, 1978). Some captive chimpanzees with injuries to digits 2 and 5 appeared to be unimpaired when knuckle-walking and some healthy individuals were observed flexing these digits so that they did not bear weight during this mode of locomotion (Tuttle, 1967). Larger captive chimpanzees have been observed using their second digit significantly less often than gorillas of equivalent size during knuckle-walking and chimpanzees of all sizes used their fifth digit significantly less often, and loaded it less than gorillas did (Inouye, 1994; Wunderlich & Jungers, 2009; Matarazzo, 2013a,b). Matarazzo (2013a,b) found the third digit regularly lifted-off last during 'palm-back' knuckle-walking in captive chimpanzees and that peak pressure was often experienced by the third digit. Wunderlich & Jungers (2009) also found that peak pressures

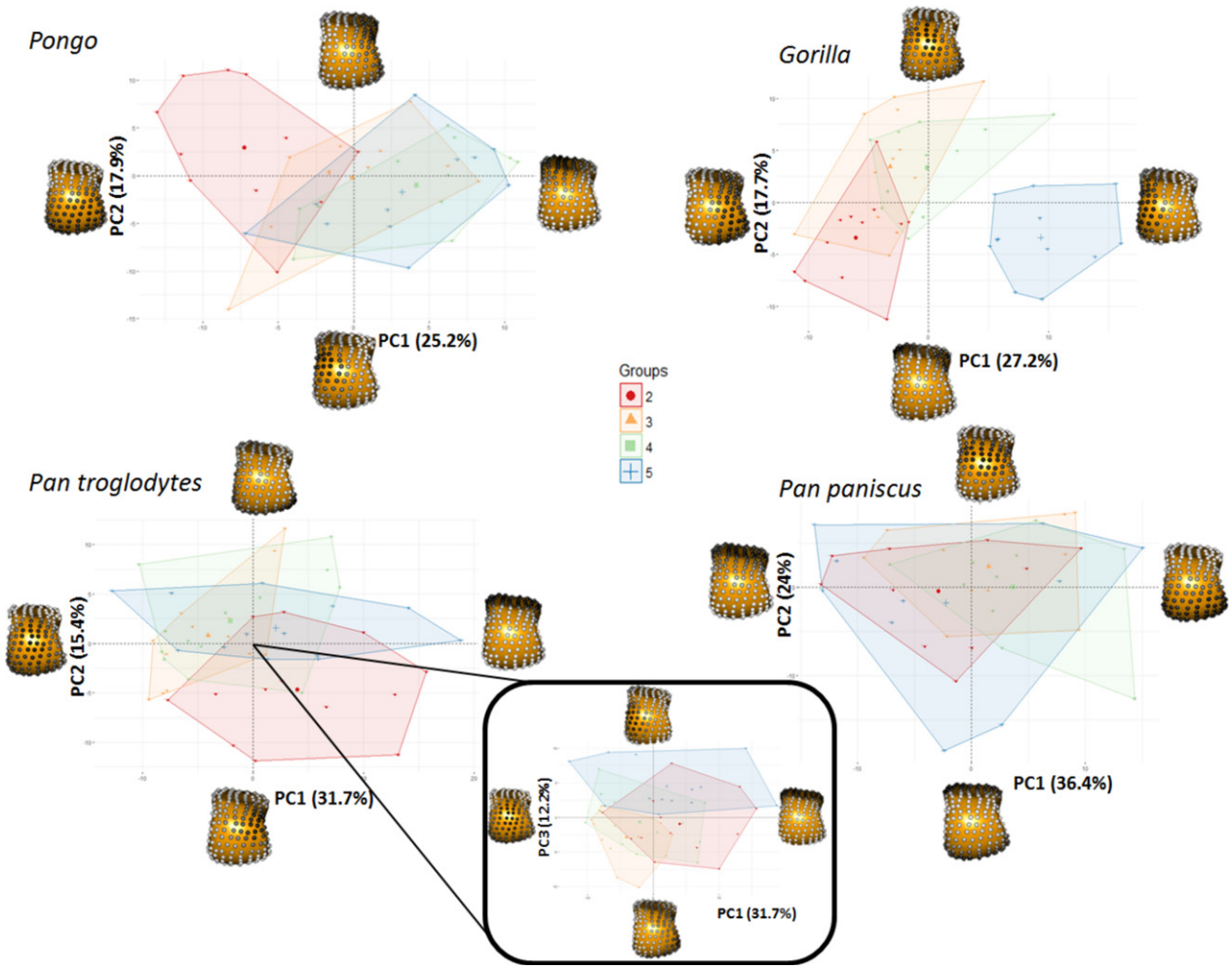

Fig. 10 RBV/TV PCA plots showing ray differences within each species. Each plot shows the first two principle components (PC) in each species, except for *Pan troglodytes*, where PC3 is depicted with PC1 (inset), as PC2 and PC3 explain a similar amount of the variance (15 and 12%, respectively) in this case. Landmarks at each extreme of a PC are coloured in greyscale, according to their signed contribution to that PC and plotted on a Mc3 in distal view. White landmarks indicate the highest signed contribution to the PC and black the least.

were higher on digits 3 and 4 than on digits 2 and 5 when young chimpanzees practised arboreal knuckle-walking and when they used a 'palm-back' posture during terrestrial knuckle-walking. Therefore, it could be argued that the more palmar RBV/TV distribution in Mc2 and Mc5, relative to Mc3 and Mc4, might reflect less loading in McP hyperextension during knuckle-walking and a need to flex digits 2 and 5 during arboreal grasping. Marzke & Wullstein (1996) have argued that the fifth digit should be the most flexed in diagonal power grips, known to be used by wild chimpanzees while vertically climbing (Hunt, 1991; Neufuss et al. 2017).

That being said, in previous hand pressure studies, all mature chimpanzees experienced peak pressures on digits 2–4 when terrestrially knuckle-walking, and the second digit usually lifts off during 'palm-in' knuckle-walking (Wunderlich & Jungers, 2009; Matarazzo, 2013a,b). Further, the second digit should be the most extended during diagonal power grips (Marzke & Wullstein, 1996), which is in contradiction to the relative flexion thought to be indicated here by the relatively palmar RBV/TV pattern found in the chimpanzee Mc2 head. Therefore, in the absence of kinematic and kinetic studies of locomotor hand postures in wild chimpanzees, we suggest that this pattern may reflect more varied hand postures and distribution of pressure across the digits during knuckle-walking (Wunderlich & Jungers, 2009; Matarazzo, 2013a,b) or more frequent arboreal grasping compared with gorillas, or a combination of both (Remis, 1995; Doran, 1996; Thorpe & Crompton, 2006).

Pan paniscus

Given the general similarities in locomotion and hand use between chimpanzees and bonobos, we predicted that bonobos would have a RBV/TV pattern that was very similar to that of chimpanzees, but with a more homogenised distribution of RBV/TV within each metacarpal head. Our

results supported these predictions; bonobos showed disto-dorsally higher RBV/TV that was more distally-extended than in gorillas and more dorsally concentrated than that of orangutans (Figs 3, 7 and 9). Bonobos differed from chimpanzees in that they possessed almost no significant inter-ray differences and they showed the most landmarks closest to the mean of BV/TV throughout the trabecular surface of each head (i.e. RBV/TV being ~ 1; Figs 3, 5 and 10). This RBV/TV distribution is consistent with the expectation raised by Tsegai et al. (2013) that bonobos would have an intermediate Mc3 trabecular structure between that of African apes and Asian apes (Fig. 9), and the intermediate thickness of Mc3 cortical bone in this species (Susman, 1979). If the relatively higher dorsal RBV/TV in chimpanzee Mc3 and Mc4 is a knuckle-walking signal, then the lack of it in bonobos, as well as the significantly higher palmar RBV/TV of Mc3, may reflect either more loading of a flexed McP joint consistent with the presumed greater arboreality in this species (Alison & Badrian, 1977; Susman et al. 1980; Susman, 1984; Crompton et al. 2010) or direct palmar loading of the metacarpal head as a result of a significant amount of arboreal palmigrady (Doran, 1993; Doran & Hunt, 1996).

Trabecular anisotropy

In contrast to the RBV/TV results, the degree of anisotropy (DA) in the subchondral trabecular bone was less variable, both in interspecies and inter-ray comparisons. Interestingly, every species studied possesses higher average DA values across the most dorsal aspect of each metacarpal (Fig. 4). As this pattern also appears in orangutans, it is likely not reflective of hyper-extension of the McP during knuckle-walking but may instead reflect fewer trabeculae at the limit of the sub-articular surface. Fewer subchondral trabecular struts would reduce the variability of alignment and thus increase DA. The main significant differences in DA were found in orangutans, which were generally more anisotropic than any other taxon, especially gorillas (Figs 4, 6, S2 and S3, Table 3). This did not support our prediction that orangutan DA would be significantly higher in the disto-palmar region, or that gorilla DA would be significantly higher in the dorsal region of the metacarpal heads compared with other hominids. Given this lack of specific regional differences it is difficult to attribute the general lack of inter-ray differences in orangutans and gorillas to functional grips as per our predictions (Figs 6 and S3). Conversely, chimpanzees and bonobos did partially support our predictions, as they showed the least significantly different landmarks in DA between them (Fig. 8) and the most inter-ray differences within each species (Fig. 6), though again it is difficult to link this to specific hand postures.

High DA in orangutans did not support our predictions and appears contradictory to previous results showing significantly lower DA in orangutans and other suspensory taxa (Tsegai et al. 2013). However, Tsegai et al. (2013) quantified and averaged trabecular DA throughout the entire Mc3 head, as opposed to just the subchondral trabeculae, which can mask the signal of higher DA in particular regions of the head. In particular, subchondral trabeculae are responsible for the initial dissipation of load from the articular, compact cortical bone through to the more internal trabecular structure in long bones such as metacarpals (Currey, 2002). Thus it may be possible that trabeculae in this region are more constrained in their orientation, as they must link the cortical shell of the metacarpal head and the deeper trabecular structure, explaining the lack of variability in DA in our sample. If this is true, the variation in DA we did find, significantly higher DA in orangutans than in other species, might be due to a general lower number of trabeculae in orangutans. However, Chirchir et al. (2017) also found that DA was consistently, if not significantly, higher in orangutans than chimpanzees in all three of their VOIs which were sampled in most of the Mc3 head. Further, higher DA has been found at the superior-central region than in other regions of the proximal *Pongo* humerus (Kivell et al. 2018). Therefore, it is unlikely that the significantly higher DA in orangutans is solely an artefact of sampling subchondral trabeculae.

High subchondral DA in orangutans may reflect a lower extension range of motion (19°) compared with that of African apes (50°) (Napier, 1960; Rose, 1988). Although orangutans have been assumed to load their hands in a greater range of postures to accommodate their diverse arboreal locomotor repertoire relative to the frequent and consistent knuckle-walking postures of African apes (Tsegai et al. 2013), the orangutan McP joint will, presumably, always been in a neutral-to-flexed posture when grasping arboreal substrates. Indeed, while variability in DA values for orangutans appears to be higher than in other taxa studied, higher average DA values are not solely driven by outlying individuals (Fig. S2) or, on further interrogation, by individuals of a particular species or sex. An analysis of trabeculae in the whole Mc3 head has reported similar intra-species variability in orangutans (Tsegai et al. 2013). Yet one constant across orangutan species and sexes is their high frequency of arboreal locomotion, requiring flexed McP grasping and perhaps a more stereotypically aligned trabecular structure, reflected in the high average DA found here. In contrast, African apes load their McP joints in both hyper-extension during knuckle-walking and a range of neutral-to-flexed postures during arboreal locomotion. The greater isotropy found within the subchondral trabeculae of African apes may reflect loading of the McP joint from multiple directions during arboreal, as well as terrestrial, behaviours.

Inferring bone functional adaptation

Many explorative comparative anatomy analyses, including the present study, can be thought of as adaptationist

(Gould & Lewontin, 1979), presenting functionally adaptive explanations for the observed data that are not easily falsified (Smith, 2016). Here, however, we submit that as the clearest differences in subchondral RBV/TV and DA patterns in the metacarpal heads are between the two species with the most disparate locomotor modes (orangutans and gorillas), and the least differences are between the two species with the most similar locomotor modes (chimpanzees and bonobos), this offers a kind of informal falsification. If the chimpanzees and bonobos were the most disparate in trabecular pattern, this would effectively falsify the broad underlying logic of our predictions. Conversely, with respect to our more specific predictions that were not confirmed, for example those regarding regional DA in *Pongo* and *Gorilla*, alternative data must be sought to explain these results (as detailed above). For example, future work that scales DA by trabecular number, analyses of the differences between subchondral and deeper trabecular structure, or detailed studies of locomotor hand postures in wild *Pongo*, could all potentially falsify some of these explanations. Nevertheless, it must be noted that the broader logic underlying more predictions holds for DA, as chimpanzees and bonobos did not display the most significant differences.

In the same vein, it could be argued that the lack of differences between chimpanzees and bonobos is due to their close phylogenetic distance rather than their similar locomotor regimes. Trabecular bone structure is controlled, at least to some extent, by genetic factors (Lovejoy et al. 2003; Havill et al. 2010; Judex et al. 2013; Almécija et al. 2015) and the role of trabecular remodelling is not solely functional (Skinner et al. 2015b); for example, trabecular bone is also important for mineral homeostasis (Clarke, 2008). There were clear differences in absolute BV/TV, however, such that bonobos demonstrated much greater subchondral BV/TV in all elements of the hand studied compared with chimpanzees (Supporting Information Fig. S7). This difference has been previously reported within the Mc3 of the same individuals in this study for which the phylogenetic influence was assessed (Tsegai et al. 2013). The relative measure used here appears to have effectively controlled for this difference in subchondral metacarpal head BV/TV. This suggests that the absolute difference in BV/TV is not functional in origin, as it is unlikely bonobos that practise a form of locomotion very similar to that of chimpanzees but with remarkably greater force. The only comparable kinematic data available demonstrate that both captive chimpanzees and captive bonobos experience similar peak pressures on their fingers during arboreal knuckle-walking (Wunderlich & Jungers, 2009; Samuel et al. 2018). If not functional in origin, the absolute difference in BV/TV between chimpanzees and bonobos may be systemic. Though a study of metatarsal trabeculae failed to find this difference in absolute BV/TV between chimpanzees and bonobos (Griffin et al. 2010), Tsegai et al. (2018) have noted that systemic differences in BV/TV between species may be variably pronounced at different anatomical sites. While the reasons for systemic differences in trabeculae might be varied, e.g. hormones, diet and disparate intestinal biomes (Tsegai et al. 2018), the difference is marked between these phylogenetically close species. As a corollary it would seem that there is little reason to suspect non-functional systematic forces are driving the similarities between RBV/TV in *Pan* species. Although the relative measure appears to have effectively controlled for possible systemic differences in subchondral trabeculae of the non-pollical metacarpal heads, there are still small differences between the species which, by process of elimination, appear to be functional in origin.

Work on intra-species variation in a large sample of a single species also supports this idea of both a systemic and functional signal in trabecular architecture. While current studies have focused on humans, likely due to the availability of specimens, data from several anatomical sites have demonstrated lower BV/TV in sedentary humans relative to mobile forager populations, primarily due to lower mechanical loading (Chirchir et al. 2015; Ryan & Shaw, 2015). Within the lower limb, this trabecular difference appears to be superimposed on a pattern of increasing trabecular gracility with increasingly distal elements of the limb (Saers et al. 2016). The transition to sedentism in human populations provides a natural experiment that allows the identification of a trabecular functional signal superimposed onto a structural limb-tapering signal, which is also found in cortical bone (Saers et al. 2016). We argue that the phylogenetic proximity and similar locomotion of *Pan* also provides a natural experiment that begins to separate functional and systemic differences between these species, as seen in the present RBV/TV results. Future work should consider the possibility of clarifying functional and systemic signals in trabecular bone.

It would be interesting to apply these methods to the pollicial metacarpal of hominids, and perhaps a larger sample of primates, in order to test for manipulative behaviour signals that may lie in the subchondral trabecular bone. Even this relatively small comparative sample may be used to contextualise fossil hominin trabeculae to shed light on their habitually loaded hand postures. Though relatively complete fossil hominin hands are rare in the archaeological record, this comparative sample demonstrates that isolated Mc2 or Mc5 elements are more important than previously thought for identifying habitual hand use in our ancestors.

Conclusion

Using a geometric morphometric approach, we demonstrated significant differences in the distribution of subchondral trabecular RBV/TV across great apes that were consistent with our predicted differences in McP joint loading during locomotion. Results of this study generally confirm previous analyses of metacarpal head trabecular

structure that have largely focused only on the Mc3, but provide for the first time a statistically robust comparison using the whole-epiphysis approach. By building upon previous work to look at trabecular structure across all of the non-pollical metacarpals, we revealed novel RBV/TV patterns in the inter-ray comparisons within *Gorilla* and *Pan* that are consistent with differences in hand posture during knuckle-walking and the frequency of arboreal locomotion. However, these inferences require testing with more detailed kinematic and kinetic analyses of the hand, ideally in wild African apes. Contrary to our predictions, we found few significant differences in DA across taxa, with *Pongo* demonstrating significantly higher DA than African ape taxa. We conclude that the interspecific variation in subchondral trabecular RBV/TV revealed here is consistent with what is currently known about great ape hand use and McP joint loading and, as such, provides a valuable comparative context in which to interpret the trabecular structure of fossil hominoid or hominin metacarpal heads.

Acknowledgements

We would like to thank Inbal Livne (Powell-Cotton Museum), Anneke van Heteren, Michael Hiermeier (Zoologische Staatssammlung München), Christophe Boesch, Uta Schwarz (MPI-EVA), and Ana Ragni (NMNH) for access to specimens. We would also like to thank David Plotzki (MPI-EVA) and Keturah Smithson (Cambridge Biotomography Centre) for assistance in scanning these specimens, as well as Matthew Tocheri for assistance with landmarking software and Leoni Georgiou for discussions that enhanced this manuscript. We are also grateful to two anonymous reviewers whose feedback greatly improved this manuscript. This research was supported by European Research Council Starting Grant #336301 (C.J.D., M.M.S., T.L.K.), the Max Planck Society and the Fyssen Foundation (A.B.).

References

Adams DC, Collyer ML, Kaliontzopoulou A, et al. (2017) Geomorph: Software for geometric morphometric analyses. R package version 3.0.5.

Alexander C (1994) Utilisation of joint movement range in arboreal primates compared with human subjects: an evolutionary frame for primary osteoarthritis. *Ann Rheum Dis* **53**, 720–725.

Alison F, Badrian N (1977) Pygmy chimpanzees. *Oryx* **13**, 463–468.

Allen MR, Burr DB (2014) Bone modeling and remodeling. In: *Basic and Applied Bone Biology* (eds Burr DB, Allen MR), pp. 75–90. London: Academic Press.

Almécija S, Wallace IJ, Judex S, et al. (2015) Comment on 'Human-like hand use in *Australopithecus africanus*'. *Science* **348**, 1101–1101.

Barak MM, Lieberman DE, Hublin JJ (2011) A Wolff in sheep's clothing: trabecular bone adaptation in response to changes in joint loading orientation. *Bone* **49**, 1141–1151.

Barak MM, Lieberman DE, Raichlen D, et al. (2013a) Trabecular evidence for a human-like gait in *Australopithecus africanus*. *PLoS ONE* **8**, e77687.

Barak MM, Lieberman DE, Hublin JJ (2013b) Of mice, rats and men: trabecular bone architecture in mammals scales to body mass with negative allometry. *J Struct Biol* **183**, 123–131.

Barak MM, Sherratt E, Lieberman DE (2017) Using principal trabecular orientation to differentiate joint loading orientation in the 3rd metacarpal heads of humans and chimpanzees. *J Hum Evol* **113**, 173–182.

Biewener AA, Fazzalari NL, Konieczynski DD, et al. (1996) Adaptive changes in trabecular architecture in relation to functional strain patterns and disuse. *Bone* **19**, 1–8.

Bookstein FL (1991) *Morphometric Tools for Landmark Data: Geometry and Biology*. Cambridge: Cambridge University Press.

Cant JG (1987) Positional behavior of female Bornean orangutans (*Pongo pygmaeus*). *Am J Primatol* **12**, 71–90.

Carlson KJ, Doran-Sheehy DM, Hunt KD, et al. (2006) Locomotor behavior and long bone morphology in individual free-ranging chimpanzees. *J Hum Evol* **50**, 394–404.

Chirchir H, Kivell TL, Ruff CB, et al. (2015) Recent origin of low trabecular bone density in modern humans. *Proc Natl Acad Sci U S A* **112**, 336–371.

Chirchir H, Zeininger A, Nakatsukasa M, et al. (2017) Does trabecular bone structure within the metacarpal heads of primates vary with hand posture? *CR Palevol* **16**, 533–544.

Cignoni P, Callieri M, Corsini M, et al. (2008) Meshlab: an open-source mesh processing tool. In: *Eurographics Italian Chapter Conference 2008*. (eds Scarano V, De Chiara R, Erra U), pp. 129–136. Salerno: Eurographics.

Clarke B (2008) Normal bone anatomy and physiology. *Clin J Am Soc Nephrol* **3**(Supplement 3), S131–S139.

Cowin SC (1986) Wolff's law of trabecular architecture at remodeling equilibrium. *J Biomech Eng* **108**, 83–88.

Crompton RH, Sellers WI, Thorpe SK (2010) Arboreality, terrestriality and bipedalism. *Philos Trans R Soc B* **365**, 3301–3314.

Currey JD (2002) *Bones: Structure and Mechanics*. Princeton: Princeton University Press.

D'Août K, Vereecke E, Schoonaert K, et al. (2004) Locomotion in bonobos (*Pan paniscus*): differences and similarities between bipedal and quadrupedal terrestrial walking, and a comparison with other locomotor modes. *J Anat* **204**, 353–361.

DeSilva JM, Devlin MJ (2012) A comparative study of the trabecular bony architecture of the talus in humans, non-human primates, and Australopithecus. *J Hum Evol* **63**, 536–551.

Doran DM (1992) The ontogeny of chimpanzee and pygmy chimpanzee locomotor behavior: a case study of paedomorphism and its behavioral correlates. *J Hum Evol* **23**, 139–157.

Doran DM (1993) Comparative locomotor behavior of chimpanzees and bonobos: the influence of morphology on locomotion. *Am J Phys Anthropol* **91**, 83–98.

Doran D (1996) Comparative positional behavior of the African apes. In: *Great Ape Societies* (eds McGrew WC, Marchant LF, Nishida T), pp. 213–224. Cambridge: Cambridge University Press.

Doran DM (1997) Ontogeny of locomotion in mountain gorillas and chimpanzees. *J Hum Evol* **32**, 323–344.

Doran DM, Hunt KD (1996) Comparative locomotor behavior of chimpanzees and bonobos. In: *Chimpanzee Cultures* (eds Wrangham RW, McGrew WC, de Waal FB, Heltne PG), pp. 93–108, Cambridge: Harvard University Press.

Doube M, Kłosowski MM, Wiktorowicz-Conroy AM, et al. (2011) Trabecular bone scales allometrically in mammals and birds. *Proc R Soc Lond B* **278**, 3067–3073.

Drapeau MS (2015) Metacarpal torsion in apes, humans, and early Australopithecus: implications for manipulatory abilities. *PeerJ* **3**, e1311.

Fernández PJ, Almécija S, Patel BA, et al. (2015) Functional aspects of metatarsal head shape in humans, apes, and Old World monkeys. *J Hum Evol* **86**, 136–146.

Friston KJ, Holmes AP, Worsley KJ, et al. (1995) Statistical parametric maps in functional imaging: a general linear approach. *Hum Brain Mapp* **2**, 189–210.

Frost HM (1987) Bone 'mass' and the 'mechanostat': a proposal. *Anat Rec (Hoboken)* **219**, 1–9.

Georgiou L, Kivell TP, Skinner M (2018) Trabecular bone patterning in the hominoid distal femur. *PeerJ* **6**, e5156.

Gould SJ, Lewontin RC (1979) The spandrels of San Marco and the Panglossian paradigm: a critique of the adaptationist programme. *Proc R Soc Lond Ser B* **205**, 581–598.

Griffin N, D'Août K, Ryan T, et al. (2010) Comparative forefoot trabecular bone architecture in extant hominids. *J Hum Evol* **59**, 202–213.

Gross T, Kivell TL, Skinner MM, et al. (2014) A CT-image-based framework for the holistic analysis of cortical and trabecular bone morphology. *Palaeontol Electronica* **17**, 1.

Gunz P, Mitteroecker P (2013) Semilandmarks: a method for quantifying curves and surfaces. *Hystrix* **24**, 103–109.

Gunz P, Mitteroecker P, Bookstein FL (2005) Semilandmarks in three dimensions. In: *Modern Morphometrics in Physical Anthropology* (ed. Slice DE), pp. 73–98. Boston: Springer.

Havill L, Allen M, Bredbenner T, et al. (2010) Heritability of lumbar trabecular bone mechanical properties in baboons. *Bone* **46**, 835–840.

Hunt K (1991) Mechanical implications of chimpanzee positional behavior. *Am J Phys Anthropol* **86**, 521–536.

Hunt K (2004) The special demands of great ape locomotion and posture. In: *The Evolution of Thought: Evolutionary Origins of Great Ape Intelligence* (eds Begun D, Russon A), pp. 172–189. Cambridge: Cambridge University Press.

Hunt KD (2016) Why are there apes? Evidence for the co-evolution of ape and monkey ecomorphology. *J Anat* **228**, 630–685.

Hunt KD, Cant JG, Gebo DL, et al. (1996) Standardized descriptions of primate locomotor and postural modes. *Primates* **37**, 363–387.

Inouye SE (1992) Ontogeny and allometry of African ape manual rays. *J Hum Evol* **23**, 107–138.

Inouye S (1994) Ontogeny of knuckle-walking hand postures in African apes. *J Hum Evol* **26**, 459–485.

Jones E, Oliphant T, Peterson P (2001) SciPy: open source scientific tools for Python. http://www.scipy.org/.

Judex S, Zhang W, Donahue LR, et al. (2013) Genetic loci that control the loss and regain of trabecular bone during unloading and reambulation. *J Bone Miner Res* **28**, 1537–1549.

Kazhdan M, Hoppe H (2013) Screened Poisson surface reconstruction. *ACM Trans Graph* **23**, 29–42.

Kivell TL, Skinner MM, Lazenby R, et al. (2011) Methodological considerations for analyzing trabecular architecture: an example from the primate hand. *J Anat* **218**, 209–225.

Kivell TL, Davenport R, Hublin JJ, et al. (2018) Trabecular architecture and joint loading of the proximal humerus in extant hominoids, Ateles, and *Australopithecus africanus*. *Am J Phys Anthropol* **167**, 348–365.

Lambers FM, Koch K, Kuhn G, et al. (2013a) Trabecular bone adapts to long-term cyclic loading by increasing stiffness and normalization of dynamic morphometric rates. *Bone* **55**, 325–334.

Lambers FM, Bouman AR, Rimnac CM, et al. (2013b) Microdamage caused by fatigue loading in human cancellous bone: relationship to reductions in bone biomechanical performance. *PLoS ONE* **8**, e83662.

Lazenby R, Skinner M, Hublin J, et al. (2011) Metacarpal trabecular architecture in the chimpanzee (*Pan troglodytes*): evidence for locomotion and tool use. *Am J Phys Anthropol* **144**, 215–225.

Lewis OJ (1977) Joint remodelling and the evolution of the human hand. *J Anat* **123**, 157–201.

Lovejoy CO, McCollum MA, Reno PL, et al. (2003) Developmental biology and human evolution. *Annu Rev Anthropol*, **32**, 85–109.

Manduell KL, Morrogh-Bernard HC, Thorpe SK (2011) Locomotor behavior of wild orangutans (*Pongo pygmaeus wurmbii*) in disturbed peat swamp forest, Sabangau, Central Kalimantan, Indonesia. *Am J Phys Anthropol* **145**, 348–359.

Marchi D, Proctor DJ, Huston E, et al. (2017) Morphological correlates of the first metacarpal proximal articular surface with manipulative capabilities in apes, humans and South African early hominins. *CR Palevol* **16**, 645–654.

Martin RB, Burr DB, Sharkey NA (1998) *Skeletal Tissue Mechanics*. New York: Springer.

Marzke MW, Wullstein KL (1996) Chimpanzee and human grips: a new classification with a focus on evolutionary morphology. *Int J Primatol* **17**, 117–139.

Marzke MW, Wullstein KL, Viegas SF (1992) Evolution of the power ('squeeze') grip and its morphological correlates in hominids. *Am J Phys Anthropol* **89**, 283–298.

Matarazzo SA (2013a) Manual pressure distribution patterns of knuckle-walking apes. *Am J Phys Anthropol* **152**, 44–50.

Matarazzo SA (2013b) Knuckle-Walking Signal in the Manual Phalanges and Metacarpals of the Great Apes (*Pan* and *Gorilla*) (Vol. Paper 755). UMass Amherst: PhD thesis.

Matarazzo SA (2015) Trabecular architecture of the manual elements reflects locomotor patterns in primates. *PLoS ONE* **10**, e0120436.

Napier JR (1960) Studies of the hands of living primates. *J Zool* **134**, 647–657.

Neufuss J, Robbins MM, Baeumer J, et al. (2017) Comparison of hand use and forelimb posture during vertical climbing in mountain gorillas (*Gorilla beringei beringei*) and chimpanzees (*Pan troglodytes*). *Am J Phys Anthropol* **164**, 651–664.

Niewoehner WA (2005) A geometric morphometric analysis of Late Pleistocene human metacarpal 1 base shape. In: *Modern Morphometrics in Physical Anthropology* (ed. Slice DE), pp. 285–298, Boston, MA: Springer.

Odgaard A, Kabel J, van Rietbergen B, et al. (1997) Fabric and elastic principal directions of cancellous bone are closely related. *J Biomech* **30**, 487–495.

Oksanen J, Blanchet F, Friendly M, et al. (2018) vegan: Community Ecology Package.

Orr CM (2016) Functional morphology of the primate hand: recent approaches using biomedical imaging, computer modeling, and engineering methods. In: *The Evolution of the Primate Hand* (eds Kivell T, Lemelin P, Richmond B, Schmitt D), pp. 227–257. New York: Springer.

Pahr DH, Zysset PK (2009) From high-resolution CT data to finite element models: development of an integrated modular

framework. *Comput Methods Biomech Biomed Engin* **12**, 45–57.

Pontzer H, Lieberman DE, Momin E, et al. (2006) Trabecular bone in the bird knee responds with high sensitivity to changes in load orientation. *J Exp Biol* **209**, 57–65.

R Core Development Team (2016) R: A language and environment for statistical computing. Vienna: R Foundation for Statistical Computing.

Rein TR (2018) A geometric morphometric examination of hominoid third metacarpal shape and its implications for inferring the precursor to terrestrial bipedalism. Anat Rec (Hoboken) https://doi.org/10.1002/ar.23985.

Remis M (1995) Effects of body size and social context on the arboreal activities of lowland gorillas in the Central African Republic. *Am J Phys Anthropol* **97**, 413–433.

Remis M (1998) The gorilla paradox: the effects of body size and habitat on the positional behavior of lowland and mountain gorillas. In: *Primate Locomotion* (eds Stasser E, Fleagle J, Rosenberge A, McHenry H), pp. 95–106. Boston: Springer.

Rodman P (1984) Foraging and social systems of orangutans and chimpanzees. In: *Adaptations for Foraging in Non-Human Primates* (eds Rodman P, Cant J), pp. 134–160. New York: Columbia University.

Rolian C, Lieberman DE, Hallgrímsson B (2010) The coevolution of human hands and feet. *Evolution* **64**, 1558–1568.

Rose MD (1988) Functional anatomy of the cheiridia. In: *Orangutan Biology* (ed. Schwartz J), pp. 299–310. Oxford: Oxford University Press.

Ruff CB, Runestad JA (1992) Primate limb bone structural adaptations. *Annu Rev Anthropol*, **21**, 407–433.

Ryan TM, Shaw CN (2013) Trabecular bone microstructure scales allometrically in the primate humerus and femur. *Proc R Soc Lond B* **280**, 20130172.

Ryan TM, Shaw CN (2015) Gracility of the modern *Homo sapiens* skeleton is the result of decreased biomechanical loading. *Proc Natl Acad Sci U S A* **112**, 372–377.

Ryan TM, Walker A (2010) Trabecular bone structure in the humeral and femoral heads of anthropoid primates. *Anat Rec (Hoboken)* **293**, 719–729.

Ryan TM, Carlson KJ, Gordon AD, et al. (2018) Human-like hip joint loading in *Australopithecus africanus* and *Paranthropus robustus*. *J Hum Evol* **121**, 12–24.

Saers JP, Cazorla-Bak Y, Shaw CN, et al. (2016) Trabecular bone structural variation throughout the human lower limb. *J Hum Evol* **97**, 97–108.

Samuel DS, Nauwelaerts S, Stevens JM, et al. (2018) Hand pressures during arboreal locomotion in captive bonobos (*Pan paniscus*). *J Exp Biol*, **221**, e170910.

Sarmiento EE (1988) Anatomy of the hominoid wrist joint: its evolutionary and functional implications. *Int J Primatol* **9**, 281–345.

Sarmiento EE (1994) Terrestrial traits in the hands and feet of gorillas. *Am Mus Novit* **3091**, 1–56.

Sarringhaus LA, Stock JT, Marchant LF, et al. (2005) Bilateral asymmetry in the limb bones of the chimpanzee (*Pan troglodytes*). *Am J Phys Anthropol* **128**, 840–845.

Scherf H, Tilgner R (2009) A new high-resolution computed tomography (CT) segmentation method for trabecular bone architectural analysis. *Am J Phys Anthropol* **140**, 39–51.

Scherf H, Wahl J, Hublin JJ, et al. (2016) Patterns of activity adaptation in humeral trabecular bone in Neolithic humans and present-day people. *Am J Phys Anthropol* **159**, 106–115.

Schlager S (2017) Morpho and Rvcg-shape analysis in R: R-packages for geometric morphometrics, shape analysis and surface manipulations. In: *Statistical Shape and Deformation Analysis: Methods, Implementation and Applications* (eds Zheng G, Li S, Székely G), pp. 217–256. Cambridge: Academic Press.

Schmitt D, Zeininger A, Granatosky MC (2016) Patterns, variability, and flexibility of hand posture during locomotion in primates. In: *The Evolution of the Primate Hand* (eds Kivell T, Lemelin P, Richmond B, Schmitt D), pp. 345–369. New York: Springer.

Skinner MM, Stephens NB, Tsegai ZJ, et al. (2015a) Human-like hand use in *Australopithecus africanus*. *Science* **347**, 395–399.

Skinner MM, Stephens NB, Tsegai ZJ, et al. (2015b) Response to comment on 'Human-like hand use in Australopithecus africanus'. *Science* **348**, 1101.

Smith RJ (2016) Explanations for adaptations, just-so stories, and limitations on evidence in evolutionary biology. *Evol Anthropol* **25**, 276–287.

Stephens NB, Kivell TL, Gross T, et al. (2016) Trabecular architecture in the thumb of *Pan* and *Homo*: implications for investigating hand use, loading, and hand preference in the fossil record. *Am J Phys Anthropol* **161**, 603–619.

Stephens NB, Kivell TL, Pahr DH, et al. (2018) Trabecular bone patterning across the human hand. *J Hum Evol*, **123**, 1–23.

Su A, Wallace IJ, Nakatsukasa M (2013) Trabecular bone anisotropy and orientation in an Early Pleistocene hominin talus from East Turkana, Kenya. *J Hum Evol* **64**, 667–677.

Sugardjito J, Cant JG (1994) Geographic and sex differences in positional behavior of orang-utans. *Treubia* **31**, 31–41.

Sugardjito J, van Hooff J (1986) Age-sex class differences in the positional behavior of the Sumatran orangutan (*Pongo pygmaeus abelii*) in the Gunung Leuser National Park, Indonesia. *Folia Primatol* **47**, 14–25.

Susman RL (1979) Comparative and functional morphology of hominoid fingers. *Am J Phys Anthropol* **50**, 215–236.

Susman RL (1984) The locomotor behavior of *Pan paniscus* in the Lomako Forest. In: *The Pygmy Chimpanze* (ed. Susman RL), pp. 369–393. Boston: Springer.

Susman RL, Badrian NL, Badrian AJ (1980) Locomotor behaviour of *Pan paniscusin* Zaire. *Am J Phys Anthropol* **53**, 69–80.

Sylvester AD, Terhune CE (2017) Trabecular mapping: leveraging geometric morphometrics for analyses of trabecular structure. *Am J Phys Anthropol* **163**, 553–569.

Thompson NE, Ostrofsky KR, McFarlin SC, et al. (2018) Unexpected terrestrial hand posture diversity in wild mountain gorillas. *Am J Phys Anthropol* **166**, 84–94.

Thorpe SK, Crompton RH (2005) Locomotor ecology of wild orangutans (*Pongo pygmaeus abelii*) in the Gunung Leuser Ecosystem, Sumatra, Indonesia: A multivariate analysis using log-linear modelling. *Am J Phys Anthropol* **127**, 58–78.

Thorpe SK, Crompton RH (2006) Orangutan positional behavior and the nature of arboreal locomotion in Hominoidea. *Am J Phys Anthropol* **131**, 384–401.

Tsegai ZJ, Kivell TL, Gross T, et al. (2013) Trabecular bone structure correlates with hand posture and use in hominoids. *PLoS ONE* **8**, e78781.

Tsegai ZJ, Stephens NB, Treece GM, et al. (2017) Cortical bone mapping: an application to hand and foot bones in hominoids. *CR Palevol* **16**, 690–701.

Tsegai ZJ, Skinner MM, Pahr DH, et al. (2018) Systemic patterns of trabecular bone across the human and chimpanzee skeleton. *J Anat*, **232**, 641–656.

Tuttle RH (1967) Knuckle-walking and the evolution of hominoid hands. *Am J Phys Anthropol* **26**, 171–206.

Tuttle RH, Basmajian JV (1978) Electromyography of pongid shoulder muscles. III. Quadrupedal positional behavior. *Am J Phys Anthropol*, **49**, 57–69.

Tuttle RH, Watts DP (1985) The positional behavior and adaptive complexes of Pan (Gorilla). In: *Primate Morphophysiology, Locomotor Analyses and Human Bipedalism* (ed. Kondo S), pp. 261–288. Tokyo: University of Tokyo Press.

Uchiyama T, Tanizawa T, Muramatsu H, et al. (1999) Three-dimensional microstructural analysis of human trabecular bone in relation to its mechanical properties. *Bone* **25**, 487–491.

Wunderlich RE, Jungers WL (2009) Manual digital pressures during knuckle-walking in chimpanzees (*Pan troglodytes*). *Am J Phys Anthropol* **139**, 394–403.

Yeh HC, Wolf BS (1977) Radiographic anatomical landmarks of the metacarpo-phalangeal joints. *Radiology* **122**, 353–355.

Zeininger A, Richmond BG, Hartman G (2011) Metacarpal head biomechanics: a comparative backscattered electron image analysis of trabecular bone mineral density in *Pan troglodytes*, *Pongo pygmaeus*, and *Homo sapiens*. *J Hum Evol* **60**, 703–710.

Zeininger A, Patel BA, Zipfel B, et al. (2016) Trabecular architecture in the StW 352 fossil hominin calcaneus. *J Hum Evol* **97**, 145–158.

Zhou G-Q, Pang Z-H, Chen Q-Q, et al. (2014) Reconstruction of the biomechanical transfer path of femoral head necrosis: a subject-specific finite element investigation. *Comput Biol Med* **52**, 96–101.

Zihlman AL (1984) Body build and tissue composition in *Pan paniscus* and *Pan troglodytes*, with comparisons to other hominoids. In: *The Pygmy Chimpanzee* (ed. Susman RL), pp. 179–200. Boston: Springer.

Supporting Information

Additional Supporting Information may be found in the online version of this article:

Fig. S1. Repeatability tests of landmarks.

Fig. S2. DA plots showing species differences within each metacarpal head.

Fig. S3. DA PCA plots showing ray differences within each species.

Fig. S4 A captive orangutan engaged in a diagonal 'double-locked' grip around a piece of string.

Fig. S5. *Gorilla* average RBV/TV by sex, mapped to average models of right Mc heads in distal view for (A) Male Mc5, (B) Male Mc2, (C) Female Mc5 and (D) Female Mc2, specimens. Note that the radio-ulnar bias is present in both sexes (see main text for details).

Fig. S6. Landmark template projected onto Mc3s of individual (A) *Gorilla gorilla*, (B) *Pan troglodytes,* (C) *Pan paniscus* and (d) *Pongo pygmaeus* specimens.

Fig. S7. Species average absolute BV/TV, mapped to average models of each Mc head in (A) distal, (B) palmar and (C) dorsal views.

Table S1. Descriptive statistics of absolute *Z*-scores from significant pair-wise inter-species landmark comparisons.

Table S2. Descriptive statistics of absolute *Z*-scores from significant pair-wise inter-ray landmark comparisons.